# REPORT DOCUMENTATION PAGE

Form Approved
OMB No. 0704-0188



| 1. AGENCY USE ONLY (Leave blank) | 2. REPORT DATE | 3. REPORT TYPE AND DATES COVERED |
|---|---|---|
| | | FINAL/27 Sep 91 to 01 Mar 95 |

**4. TITLE AND SUBTITLE**
APPLICATION OF WAVELETS TO AUTOMATIC TARGET RECOGNITION

**5. FUNDING NUMBERS**
7450/09
F49620-91-C-0096

**6. AUTHOR(S)**
MR CHARLES STIRMAN

**7. PERFORMING ORGANIZATION NAME(S) AND ADDRESS(ES)**
MARTIN MARIETTA TECHNOLOGIES INC.
ELECTRONICS AND MISSILES
5600 SAND LAKE ROAD
ORLANDO, FLORIDA 32819-8907

**8. PERFORMING ORGANIZATION REPORT NUMBER**
AFOSR-TR- 95-0396

**9. SPONSORING/MONITORING AGENCY NAME(S) AND ADDRESS(ES)**
AFOSR/NM
110 DUNCAN AVE, SUTE B115
BOLLING AFB DC 20332-0001

**10. SPONSORING/MONITORING AGENCY REPORT NUMBER**
F49620-9-C-0096

**11. SUPPLEMENTARY NOTES**





**12a. DISTRIBUTION/AVAILABILITY STATEMENT**
APPROVED FOR PUBLIC RELEASE: DISTRIBUTION IS UNLIMITED

**12b. DISTRIBUTION CODE**

**13. ABSTRACT (Maximum 200 words)**
Contract F49620-91-C-0096, "Application of Wavelets to Automatic Target Recognition," is the second phase of multiphase project to insert compactly supported wavelets into an existing or near-team Department of Defense system such as the Longbow fire control radar for the Apache Attack Helicopter. In this contract, we have concentrated mainly on the classifier function. During the first phase of the program (Contract F49620-90-C-0050, "Application of Wavelets to Radar Data Processing"), Martin Marietta demonstrated the feasibility of using wavelets to process high range resolution profile (HRRP) amplitude returns from a wide bandwidth radar system. During this phase, Martin Marietta, with Fast Mathematical Algorithms and Hardware, Inc., as a subcontractor, obtained fully polarized wide bandwidth radar HRRP amplitude returns and procesed, them with wavelet and wavelet packet or (best basis) transforms. Then, by mathematically defined nonlinear feature selection, we showed that significant improvements in the probability of correct classification are possible, up to 14 percentage points maximum (4 percentage points average) improvement when compared to the current classifier performance. In addition, We addressed the feasibility of using wavelet packets' best basis to address target registration, man-made object rejection, clutter discrimination, and synthetic aperture radar scenes speckle removal and object registration.



**14. SUBJECT TERMS**

**15. NUMBER OF PAGES**

**16. PRICE CODE**

| 17. SECURITY CLASSIFICATION OF REPORT | 18. SECURITY CLASSIFICATION OF THIS PAGE | 19. SECURITY CLASSIFICATION OF ABSTRACT | 20. LIMITATION OF ABSTRACT |
|---|---|---|---|
| UNCLASSIFIED | UNCLASSIFIED | UNCLASSIFIED | SAR(SAME AS REPORT) |

# Application of Wavelets to Automatic Target Recognition (ATR)

**Final Technical Report – CLIN 0002AA**
for the Period September 1991 – April 1995
Program Code OE20 & 1E20

Amount of Contract Dollars $2,161,623


**Principal Investigator**
Mr. Charles Stirman
407-356-2573

**Program Manager**
Dr. Arje Nachman
202-767-4939





**Sponsored by**
**Advanced Research Projects Agency**
**ARPA Order No. 7149/04 & 7450/02**
**Monitored by AFOSR Under Contract No. F49620-91-C-0096**



Martin Marietta Technologies, Inc.
Electronics and Missiles
5600 Sand Lake Road
Orlando, Florida 32819-8907

# Application of Wavelets to Automatic Target Recognition (ATR)

**Final Technical Report – CLIN 0002AA**
for the Period September 1991 – April 1995
Program Code OE20 & 1E20

Amount of Contract Dollars $2,161,623


**Principal Investigator**
Mr. Charles Stirman
407-356-2573

**Program Manager**
Dr. Arje Nachman
202-767-4939





**Sponsored by**
**Advanced Research Projects Agency**
**ARPA Order No. 7149/04 & 7450/02**
**Monitored by AFOSR Under Contract No. F49620-91-C-0096**



Martin Marietta Technologies, Inc.
Electronics and Missiles
5600 Sand Lake Road
Orlando, Florida 32819-8907







OR 21,102/AR045-0022

## TABLE OF CONTENTS

## LIST OF FIGURES

## LIST OF TABLES

## LIST OF ACRONYMS AND ABBREVIATIONS

| | |
|---|---|
| AFOSR | Air Force Office of Scientific Research |
| APG | Aberdeen Proving Ground |
| APP | Appendix article, 1992 Annual Technical Report |
| ARPA | Advanced Research Projects Agency |
| ATR | automatic target recognition |
| BB | similar to BD except for PM classifier |
| BD | Mahalanobis distance + ln (determinant) (i.e. Q discriminant) |
| BIAS | number added to quadrature and profile matching classifier calculations to shift |
| $P_{cc}$ | Probability of correct classification |
| BL | baseline |
| CLx | target class where x is 1, 2, 3, etc. |
| FCR | fire control radar |
| FMA&H | Fast Mathematical Algorithms and Hardware, Inc. |
| HL | Hunter-Liggett |
| HRRP | high range resolution profile |
| I | in-phase portion of coherent radar return |
| LPTRAIN | file name implying few calculations in classifier |
| M1 | equally weighted method of averaging $P_{cc}$ values |
| M2 | sample size weighted method of averaging $P_{cc}$ values |
| MMO | man-made object |
| MMW | millimeter wave |
| O/E | total odd power divided by total even power |
| $P_{cc}$ | percent correct classification |
| PM | profile matching classifier |
| PM_DELTA | measure of PM classifier's confidence |
| POP | Proof of Principle, usually referring to the preproduction Longbow FCR system |

| | |
|---|---|
| Q | quadrature component of coherent radar return |
| QD | quadratic classifier |
| Q_DELTA | measure of QD classifier's confidence |
| SAR | synthetic aperture radar |
| STD | standard deviation (large implies long target) |
| TT | target-on-turntable radar data |
| WSMR | White Sands Missile Range |
| YPG | Yuma Proving Grounds |

## SUMMARY

Contract F49620-91-C-0096, "Application of Wavelets to Automatic Target Recognition," is the second phase of a multiphase project to insert compactly supported wavelets into an existing or near-term Department of Defense system such as the Longbow fire control radar for the Apache Attack Helicopter. In this contract, we have concentrated mainly on the classifier function. During the first phase of the program (Contract F49620-90-C-0050, "Application of Wavelets to Radar Data Processing"), Martin Marietta demonstrated the feasibility of using wavelets to process high range resolution profile (HRRP) amplitude returns from a wide bandwidth radar system. During this phase, Martin Marietta, with Fast Mathematical Algorithms and Hardware, Inc., as a subcontractor, obtained fully polarized wide bandwidth radar HRRP amplitude returns and processed them with wavelet and wavelet packet (or best basis) transforms. Then, by mathematically defined nonlinear feature selection, we showed that significant improvements in the probability of correct classification are possible, up to 14 percentage points maximum (4 percentage points average) improvement when compared to the current classifier performance.

In addition, we addressed the feasibility of using wavelet packets' best basis to address target registration, man-made object rejection, clutter discrimination, and synthetic aperture radar scene speckle removal and object registration.


## I. Technical Problem

Modern airborne fire control radar (FCR) systems must provide rapid, accurate, and automatic detection and recognition of targets to flight crews in adverse weather with minimal false alarms to improve their survivability in battlefield environments. Typical automatic target recognition (ATR) algorithms for a real-beam millimeter wave (MMW) radar begin with high range resolution profiles (HRRPs) with 1- to 2-foot resolution or range cells. These HRRPs are the magnitude of the Fast Fourier Transform (FFT) coefficients of the transmitted and received wide bandwidth frequency spectrum input from each of several radar polarizations. After registration to center the HRRPs in the processing range bin, features are extracted and used in algorithms for

target/clutter discrimination, target/man-made object (MMO) rejection, and target classification, usually in that order. This processing flow is shown in Figure 1.

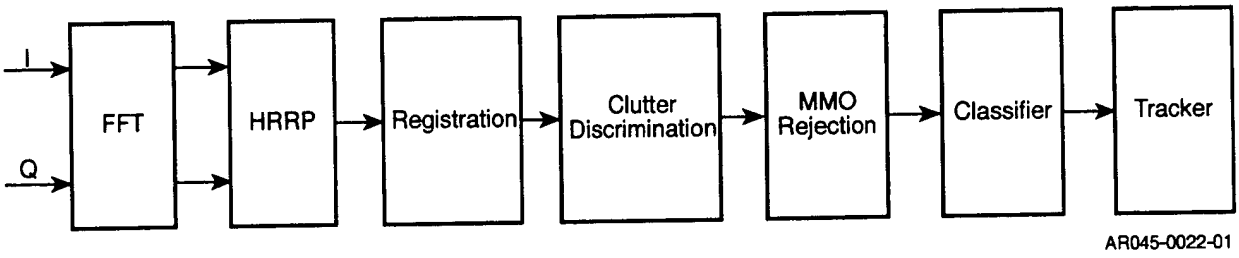


**Figure 1. High Range Resolution Processing Flow**

In most cases, the dimensionality of the feature space is large, which severely restricts practical application of pattern recognition schemes. It is expected that compactly supported wavelet transforms can be applied efficiently to compress the HRRPs while retaining relevant information, reducing feature vector dimension, and allowing more powerful ATR algorithms.

The task addressed in this effort was to show the feasibility of effectively processing full polarimetric HRRP MMW data vectors from various targets obtained from turntable and flight sensors using wavelet-based transforms. The processed vectors were then used to obtain more useful and robust wavelet feature vectors for target classification. As time allowed, we addressed applications of the methodology to favorably impact target registration, target/clutter discrimination, target/MMO rejection, and synthetic aperture radar (SAR) data processing.

## II. General Methodology

The general methodology used in this project was to first transfer wavelet and wavelet packet technology from Fast Mathematical Algorithms and Hardware (FMA&H) to Martin Marietta through interactive workshops. Then, wavelet theory was applied to an analysis of validated turntable and field-measured radar data to determine the impact of wavelet processing on radar classifier performance. The figure of merit used to measure this performance was the classifier's probability of correct classification ($P_{CC}$). To ensure comparable performance, we used the exact same training and testing data sets and compared results at each step of the wavelet-based process

with results obtained using then-current Longbow classifier algorithms. This approach ensured an accurate comparison relative to the current baseline $P_{CC}$ of the Longbow fire control radar (FCR) system. The analysis was performed on the extensive, validated Longbow radar database that consists of target-on-turntable data and data from many flight tests.

To collect turntable data, the radar was located in a roof-house overlooking the Martin Marietta radar range. The targets were mounted on the center of a turntable that rotates and tilts under operator control to give near-hemispherical signatures. As the range from the radar to the target was fixed and centered in a given range bin, it was necessary to shift the coherent return in a circular fashion within their range bins, to simulate flight data. For this data collection, the clutter was suppressed more than 20 dB below the target signature. Therefore, coherent flight clutter data collected from Ft. A.P. Hill in Maryland was coherently embedded in the target signature data at various clutter levels and ranges to simulate real flight data. This target-on-turntable database was used for the initial classifier analysis.

Flight target data with naturally occurring clutter was then added for the design, training, and testing of classifier algorithms that showed promise. That is, some flight target data was used in addition to turntable data as part of the classifier training database, and other independent flight target data became the final database for the classifier. Flight data was used exclusively for MMO algorithm design and testing (since the MMO observations were from flight data) and for target/clutter discrimination (since this analysis requires huge numbers of radar looks at different clutter scenes).

Although this report deals primarily with wavelet target classification, it also addresses the feasibility of using wavelets for target registration, target/clutter discrimination, target/MMO rejection, and SAR processing. Target registration takes HRRP range cell data and positions this data in the center of the range bin, where a range bin can be typically 64 feet long and a range cell is one foot long. Registration needs to be consistent over large clutter levels. Since target registration precedes the target/clutter discrimination, target/MMO rejection, and target classifier algorithms, improvements in registration were expected to lead to improvements in each of these

three pattern recognition areas. Wavelet processing of two-dimensional SAR images was also explored with the assistance of FMA&H to determine the feasibility of using wavelets to reduce SAR speckle (noise) and improve target registration.

## III. Technical Results

This project produced a wavelet classifier consisting of a three-class quadratic classifier that uses 48 wavelet coefficients produced by selecting 16 wavelet coefficients from the transform of the HRRP for each of three radar polarizations. Using turntable data and coherently imbedded clutter, the wavelet classifier yielded a classifier $P_{CC}$ as shown in Table 1. The wavelet value was a maximum of 12.9 percentage points higher, and when averaged over all clutter levels and target ranges, was 6.8 percentage points higher than the Longbow baseline classifier $P_{CC}$. With flight target data, the wavelet classifier yielded a classifier $P_{CC}$ that was a maximum of 14 percentage points higher, and when averaged over all clutter levels and target ranges, was 4 percentage points higher than the Longbow baseline classifier $P_{CC}$. This wavelet classifier requires only slightly more computations than the Longbow baseline classifier.

**Table 1. Summary of Improvement for Radar Classifier Using Compactly Supported Wavelets**

| Type Of Data | Improvement (%) | | |
|---|---|---|---|
| | Maximum | Average | Minimum |
| Turntable Target with Added Flight Clutter | 12.9 | 6.8 | 3 |
| Proof of Principal System Flight Data | 14.0 | 4 - 6 | +0 |
| Full Scale Development System Flight Data | TBD | TBD | TBD |

Figure 2 presents the relative $P_{CC}$ improvement in percentage points for three levels of clutter (light, moderate and heavy) and three relative ranges (close, medium and far). Clutter for the results shown in the figure was acquired from Ft. A.P. Hill. Figure 3 presents relative $P_{CC}$ improvement in percentage points using the proof of principle (POP) flight data from four sites and two relative ranges.

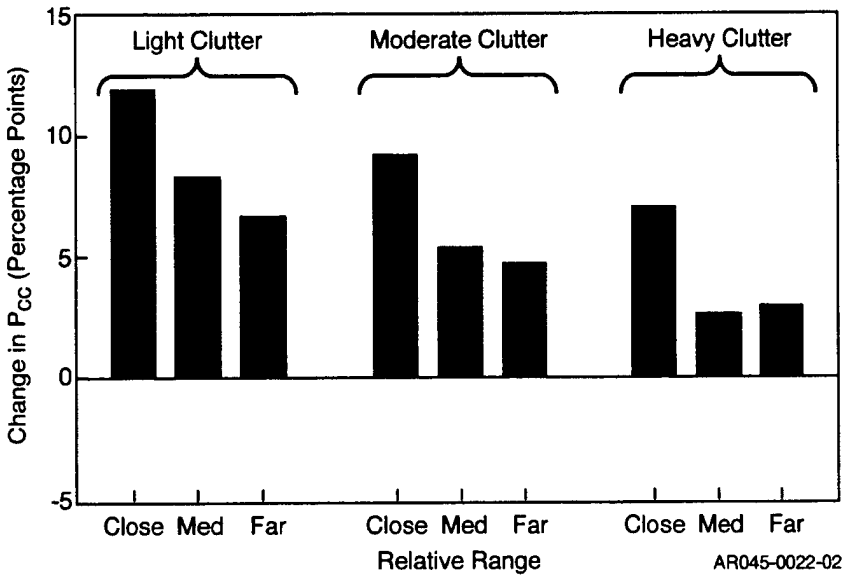


**Figure 2. Turntable Performance Enhanced by Wavelet Classifier**

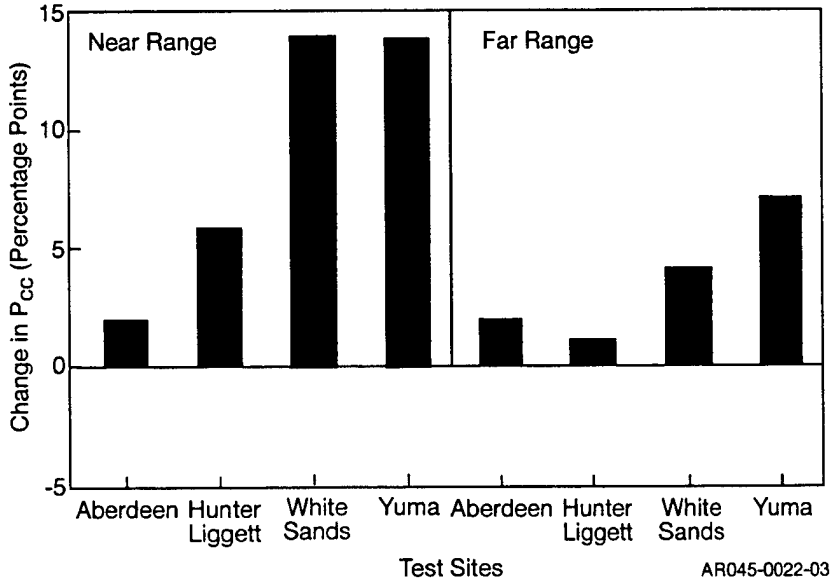


**Figure 3. Flight Data Enhanced by Wavelet Classification**

The classifier algorithms were tested against turntable target data with coherently imbedded clutter from Ft. A.P. Hill. The flight target data was acquired with the POP radar at four test sites: Aberdeen Proving Grounds (APG), Ft. Hunter-Liggett (HL), White Sands Missile Range (WSMR), and Yuma Proving Grounds (YPG). The MMO algorithms were tested against POP flight MMO and target data from the same four test sites.

The 48-dimensional wavelet quadratic classifier was tested on the Longbow flight data and at first yielded $P_{CC}$ results that were about 2 percentage points higher the Longbow baseline classifier's $P_{CC}$. Several discussions were held with FMA&H and Longbow personnel about wavelet approaches. Then, many techniques were applied to further improve this wavelet $P_{CC}$. The best approach used clustering branching logic preceding the fusion (by sensor fusion type logic) of a 42-dimensional wavelet quadratic classifier with a profile matching (nearest neighbor) classifier. Based on sample size weighting of the testing data files, this classifier yielded an average $P_{CC}$ that was 6 percentage points higher than the Longbow baseline classifier's $P_{CC}$. If the average $P_{CC}$ is computed by weighting the different target class $P_{CC}$ values equally, this wavelet classifier has a $P_{CC}$ that is 4 percentage points higher than the Longbow baseline classifier's $P_{CC}$. This wavelet classifier requires approximately the same number of computations as the Longbow baseline classifier.

One drawback to these wavelet classifiers is that they happen to be somewhat biased toward two of the three classes, at the expense of the third. That is, the $P_{CC}$ for class three tends to be lower than the $P_{CC}$ values for classes one and two. Since the Longbow baseline classifier was more balanced among the three classes, we decided to use a modified version of a wavelet fusion classifier. Using a modified version of the wavelet fusion classifier that forced a balance of the classes similar to the baseline classifier, a preliminary look showed an average $P_{CC}$ that was only 3 percentage points higher than the average baseline $P_{CC}$. This approach requires approximately the same number of computations as the Longbow baseline classifier.

Target registration prepares for pattern recognition algorithms by electronically moving the HRRP to the center of the range bin. Since registration precedes the detection and discrimination algorithms, registration algorithm performance has a great impact on the algorithms. Because significant time (several hours) is required for registration of the training data, faster methods of evaluating registration algorithms were investigated and two were defined. One wavelet registration algorithm performed better than the Longbow baseline registration method in this sense. However, this wavelet registration method dropped the average $P_{CC}$ by 1 percentage point.

The other fast method measured how well the registration method finds the known center of the turntable. In the Longbow turntable data files, the target HRRP has been randomly shifted so that the center of the HRRP is generally not the center of the turntable and different levels of clutter have been added to the target; however, it is possible to retrieve the original center of the turntable position in this shifted HRRP for registration testing purposes. An experiment was conducted where the targets were always centered in the HRRP range bin. When the Longbow baseline classifier was trained and tested on data using a registration method that always picks the true center of the turntable, an average $P_{CC}$ improvement of 9.16 percentage points resulted. Then, a second wavelet-based registration algorithm, which was also better than the Longbow baseline registration algorithm in this sense, showed some improvement in classifier average $P_{CC}$. Since this evaluation method requires about 1.5 minutes of computer time to run while the classifier requires several hours run time, it appears that this evaluation method is a suitable fast registration evaluation tool. This experiment indicated the potential for large ATR performance improvements if registration can be significantly improved, especially if the registration accurately estimates the physical center of the target.

The target MMO rejection algorithm can be considered a two-class classifier problem, with one class being non-target MMOs and the second the targets. When the 48-dimensional wavelet quadratic classifier was first applied to the two-class, target versus MMO problem, the average $P_{CC}$ for this algorithm was 4.4 percentage points higher than the Longbow MMO baseline. Using a different selection of wavelet coefficients and a few wavelet packet coefficients, a new wavelet quadratic MMO algorithm was produced with a $P_{CC}$ that was 7.5 percentage points above the Longbow baseline. This new wavelet MMO algorithm is approximately one-third as complex as the Longbow baseline MMO algorithm.

Lincoln Labs and Sandia Labs provided synthetic aperture radar (SAR) data that was processed by wavelet methods. Wavelet processing did show some capability to clean up or remove noise from SAR imagery. Also, SAR images and simulated SAR images were processed by two-dimensional wavelet transforms. The resulting coefficients were used in a wavelet target

registration algorithm to register the SAR image. This wavelet registration procedure did show promise on both the real SAR data and the simulated SAR data.

## IV. Implications for Further Research

The preliminary success of applying wavelets to the various parts of the radar signal processing, classification, and detection algorithms suggests strongly that a rigorous effort should be funded to optimize and insert wavelet-based processing into the Longbow FCR as part of their product improvement program. Further, serious analysis and application should be undertaken to extend this methodology to the other parts of the process, including the registration, MMO rejection, and clutter discrimination algorithms. Since wavelet processing has already shown significant classifier and MMO performance improvements without increased processing complexity, it is expected that similar results will be obtained for the registration and clutter discrimination algorithms. Optimizing these approaches would require investigation of additional wavelet bases and wavelet packet approaches. Tests would need to be performed using data from the production FCR system.

Wavelets show promise for data compression while conserving relevant information in an entropy sense. This characteristic implies that wavelet-based compression could permit rapid transmission of time-critical data over existing data links. Also, additional measures of merit that are correlated with $P_{CC}$ should be sought.

The need for real-time battle damage assessment from SAR imagery could benefit from the automatic processing that wavelet-based techniques might allow.

# 1.0 INTRODUCTION

This report covers the second phase of a multiphase project. The goal was to design wavelet-based ATR algorithms for radar pattern recognition requirements that advance the state of the art in terms of improved pattern recognition performance. The Longbow FCR ATR tasks were specifically targeted due to the willingness of the Longbow Program Office to allow use of its extensive database of radar looks at targets, clutter, and man-made objects to see what ATR improvements wavelet processing may offer.

ATR for a real-beam MMW radar typically begins with the generation of HRRPs from each of several radar polarizations (Einstein [6]). Typically, these HRRPs are created by processing a finite sequence of in-phase (I) and quadrature (Q) numbers as complex numbers through a Fast Fourier Transform (FFT) and computing the magnitudes of the complex numbers output from the FFT. Features are extracted from these HRRPs and then used in algorithms for target/clutter discrimination, target/MMO discrimination, and target classification, usually in that order. It was hypothesized and demonstrated during this contract that compactly supported wavelets can efficiently retain the information in the HRRPs, while reducing feature vector dimension, and allow more powerful ATR algorithms. This approach is described in Section 3.0.

A general ATR scheme is depicted in Figure 4. Feature extraction in the upper sequence represents the conversion from raw radar input ($\overline{x}$) to the set of features ($\overline{y}$) to be used in the classifier stage of the algorithm. Conversion from observation space to feature space is the function of feature extraction. Once the data is in feature space, it can be processed in the classifier. The classifier's function is to decide between the various target types (e.g., Target A vs. Target B vs. Target C). The wavelet transform is an alternative means of performing feature extraction yielding a new set of wavelet-based features ($\overline{w}$) that are added to the process. This transform is shown in the lower sequence of the figure.

The theory of wavelets and important wavelet references are discussed in Section 2.0. The wavelet ATR project was to compress HRRP data vectors to more useful wavelet-based feature vectors for target/clutter discrimination, target/MMO discrimination, and target classification.

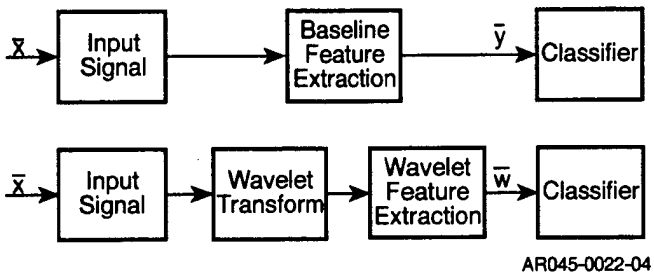


**Figure 4. Wavelet Transform as Feature Extraction**

Specifically, the project was to investigate applications of wavelet processing that could favorably impact any or all of these pattern recognition problems.

Converting to wavelets is similar to performing a Fourier transform. When the discrete Fourier transform is applied to a vector of data, the results represent the vector in the space of complex exponentials, i.e., the complex exponential functions are used as the basis functions. This says that the vector of original data can be represented as a linear combination of the complex exponentials. Converting to wavelets is an analogous operation. The original data vector is given a representation in a wavelet space and therefore can be represented as a linear combination of wavelets, rather than as a linear combination of complex exponentials as with the Fourier Transform. Part of the difference between using the complex exponentials and wavelets is the types of properties wavelets exhibit. By making a judicious choice of wavelets, the data vector can be adequately represented with fewer terms (or features). This reduction in features can be exploited in the classifier stage. The technical problem is to use wavelets in an efficient representation of targets and exploit this to improve overall radar ATR performance.

Two general types of classifier algorithms used in this project are the quadratic (QD) classifier and the profile matching (PM) classifier (also called nearest neighbor classifier). These two types of classifiers are described in Sections 3.1 and 3.3. A type of logic that originated in sensor fusion ATR work was also explored. The idea is to use sensor fusion logic to combine a QD classifier with a PM classifier even though both QD and PM originate from the same radar sensor.

If both the QD and PM are good, but not optimal classifiers, the fusion version of the two may produce better performance than either classifier alone. Wavelet processing may reduce the QD and PM feature vector dimensions to allow the fusion classifier to require no more computations than either original, non-wavelet QD or PM requires alone. This concept is discussed in Section 3.4.

The approach used on this project was to apply wavelet theory to the analysis of field-measured data and to study the impact of wavelet processing on performance of the Longbow fire control radar (FCR) system. This performance analysis was performed on the huge Longbow radar database that consists of target-on-turntable data and data from many flight tests. The targets in the turntable database have been shifted, in a circular fashion, within their range bins, to simulate flight data. Also, these targets have been embedded in real clutter (from flight data), at various clutter levels and at various range equivalents, to simulate real flight data. This target-on-turntable database was used for preliminary classifier analysis. Flight data was relied upon for final classifier design and testing, for MMO analysis (since the MMO observations were from flight data), and for target/clutter discrimination (since this analysis requires huge numbers of radar looks at different clutter scenes).

This report deals primarily with wavelet-based target classification, target/MMO algorithms, and a wavelet algorithm for target registration. Target registration attempts to take HRRP data and position this data in a consistent manner for additional processing by the target/clutter discrimination algorithms, the target/MMO algorithms, and the target classifier. Since target registration must precede each of these pattern recognition algorithms, improvements in target registration algorithms might lead to improvements in each of these three required pattern recognition areas. Also, this project performed a preliminary investigation of the benefits of wavelet processing of synthetic aperture radar (SAR) data by utilizing data from MIT Lincoln Labs and simulated SAR data. Wavelet processing of SAR images was explored with the goals of reducing noise, detecting targets in noise, and registering targets in noise.

## 2.0 WAVELET CONCEPTS

As part of the preparation for and execution of this contract, two workshops on wavelets, wavelet packets, multi-resolution analysis, and related topics were held at the Martin Marietta facility in Orlando, Florida. These workshops were conducted by our subcontractor Fast Mathematical Algorithms and Hardware, Inc. (FMA&H). The first workshop was held in October 1991 and featured Ronald Coifman, Victor Wickerhauser, and Stephane Mallat. The second workshop was held in October 1993. In addition to Ronald Coifman and Victor Wickerhauser, this second workshop featured David Donoho, Leonid Rudin, and Gregory Beylkin. Table 2 lists the topics for each of the workshops along with the lecturer.

**Table 2. Topics of Martin Marietta Wavelet Workshops**

| Presenter | Topic |
|---|---|
| Workshop I – October 1991 | |
| 1) Ronald Coifman | Overview of windows and frequency analysis |
| 2) Ronald Coifman | Wavelets, wavelet packets analysis (both continuous and discrete) |
| 3) Stephane Mallat | Overview of multi-resolution analysis and the dyadic wavelet transform |
| 4) Stephane Mallat | Two-dimensional transforms and dyadic algorithms |
| 5) Stephane Mallat | Wave1 multi-resolution software and its use |
| 6) Ronald Coifman | The Haar System, the Haar-Walsh Library and best basis |
| 7) Victor Wickerhauser | WP software description and philosophy |
| 8) Victor Wickerhauser | One- and two-dimensional transform software and technical issues |
| 9) Ronald Coifman | Applications of the best basis to one-dimensional (radar) processing |
| | |
| Workshop II – October 1993 | |
| 1) Ronald Coifman | Review of wavelets and best basis and the AWA software |
| 2) Leonid Rudin | Image enhancement, segmentation, and decluttering optical images |
| 3) Victor Wickerhauser | Basis of wavelet selection and high resolution compression |
| 4) David Donoho | Soft threshold and nonlinear denoising methods |
| 5) Gregory Beylkin | Fast synthetic aperture radar methods from seismology |
| 6) Victor Wickerhauser | Fast principal components methods and new tools |
| 7) Ronald Coifman | Advanced ATR applications |

## 2.1 Fundamental Ideas

### 2.1.1 Preliminary Concepts

Several preliminary concepts must be understood to describe wavelets. A basis of a vector space V is a set of vectors $\{\bar{u}_n\}$ which span the vector space V and are linearly independent. The set spans the space if every vector $\bar{v} \in V$ can be written as a linear combination of the vectors $\{\bar{u}_n\}$. The set $\{\bar{u}_n\}$ is linearly independent, which means that if $\Sigma c_n \bar{u}_n = 0$ then $c_n = 0$ for all i. An inner product on a vector space V is a function that assigns a scalar to each ordered pair of vectors $(\bar{u}, \bar{v})$ with the following properties:

a) $(\bar{u} + \bar{v}, \bar{w}) = (\bar{u}, \bar{w}) + (\bar{v}, \bar{w})$

b) $(c\,\bar{u}, \bar{v}) = c\,(\bar{u}, \bar{v})$

c) $(\bar{v}, \bar{u}) = \overline{(\bar{u}, \bar{v})}$, the bar denotes complex conjugation

d) $(\bar{u}, \bar{u}) > 0$, if $\bar{u} \neq 0$.

An inner product space is a vector space together with a specified inner product on that space. The positive square root of $(\bar{u}, \bar{u})$ is called the norm of $\bar{u}$, and denoted by $\| \bar{u} \|$. So, an inner product extends the usual vector dot product, and the norm of a vector extends the notion of size or length. A sequence of vectors $\{\bar{u}_n\}$ is said to converge to the limit vector $\bar{u}$ if $\lim_{n \Rightarrow \infty} \| \bar{u}n - \bar{u} \| = 0$; in this case, we write $\bar{u} \Rightarrow \bar{u}$ in norm. A sequence $\{\bar{u}_n\}$ is a Cauchy sequence if for every $\varepsilon > 0$ there exists an $N_0$ such that $\| \bar{u}_n - \bar{v}_m \| < \varepsilon$ whenever $m,n > N_0$. If for every convergent Cauchy sequence of vectors $\{\bar{u}_n\}$ the limit vector $\bar{u}$ is in V, then V is called complete. A complete inner product space is called a Hilbert space. For example, the n-dimensional real vector space $R^n$ is a Hilbert space with the usual inner product. Also, the space of Lebesgue square integrable functions on the interval [0,1], $L^2[0,1]$, is a Hilbert space with the inner product defined by $(f,g) = \int f(x)\, \overline{g(x)}\, dx$.

Two vectors are said to be orthogonal if $(\bar{u}, \bar{v}) = 0$ and we write $u \perp v$. A set of vectors, $S = \{..., \bar{u}_{-1}, \bar{u}_0, \bar{u}_1, ...\}$, is said to be orthonormal if $(\bar{u}_i, \bar{u}_j) = \delta_{ij}$, where $\delta_{ij}$ is zero unless $i = j$ when it is one. The standard basis of $R^n$ is orthonormal with the standard inner product. The set $\{\exp(2\pi int)\}$, for $n \in Z$, is an orthonormal set in $L^2[0,1]$. A linear manifold in a Hilbert space

V is a subset of V which is itself a vector space, say W. The orthogonal complement of a set W in V is the set of all vectors that are orthogonal to each of the vectors in W. We write this as $W\perp$. If W is a linear manifold, we can write a vector $\bar{v} \in V$ as $\bar{v} = \bar{w} + \bar{x}$ where $\bar{w} \in W$ and $\bar{x} \in W\perp$ . We call this projection the orthogonal projection of V onto W. A basis for the space V which is also orthonormal is called an orthonormal basis. For an orthonormal basis $\{\bar{u}_n\}$, we may write a vector $\bar{v} \in V$ as a combination of generalized Fourier Coefficients $\bar{v} = \Sigma\, c_n\, \bar{u}_n$, where $c_n = (\bar{v},\ \bar{u}_n)$ are the generalized Fourier coefficients and the series converges in norm. For $x \in L^2(R)$ (finite energy signals), this says the generalized Fourier coefficients form a finite energy sequence $(..., (x,u_{-1}), (x,u_0), (x,u_1), ...\}$ which is in $l^2(Z)$. The space $l^2(Z)$ consists of sequences $\{x_n\}$ with $\Sigma\, |x_n|^2 < \infty$. A Hilbert space which possesses a countable orthonormal basis is called separable. All separable Hilbert spaces are isomorphic (equivalent) to $l^2(Z)$. A collection $\phi_{m,\,n}$ is an unconditional basis for $V_m$, if the closure of the linear span of $\{\phi_{m,n},\ n \in Z\} = V_m$ and there exists A, B such that $0 < A \le B < \infty$ and for all $\{c_n\} \in l^2\,(z)$,

$$A\, \Sigma\, \|c_n\|^2 \le \|\Sigma\, c_n\, \phi_{m,n}\|^2 \le B\, \Sigma\, \|c_n\|^2.$$

The closure of a set is the smallest closed set containing that set.

### 2.1.2 Wavelets from a Multi-Resolution Viewpoint

With these preliminary concepts defined, we may proceed with the discussion of wavelets from a multi-resolution viewpoint. The concept of a multi-resolution analysis is based on a sequence of approximations to a function f, with each approximation being averages on different scales. If an approximation at resolution level $V_0$ is known and more detail is desired, then the projection onto $W_0$ will provide the additional information. The contribution from $W_0$ will consist of a linear combination of the wavelet basis in that space. So, we arrive at more and more detail in our representation by using the wavelet bases from the collection of $W_m$ spaces. A multi-resolution analysis (Mallat [7,8]) on $L^2(R)$ consists of:

1) A sequence of subspaces of $L^2(R)$

$$... V_2 \subset V_1 \subset V_0 \subset V_{-1} \subset V_{-2} ... \text{ such that}$$

2) $\cap V_m = \{0\}$, closure $(\cup V_m) = L^2(R)$

3) $f(\bullet) \in V_m \Leftrightarrow f(2\bullet) \in V_{m-1}$

4) there is a function, $\phi \in V_0$, so that for each $m \in Z$ the set $\{\phi_{m,n}\}$, where

$\phi_{m,n}(t) = 2^{-m/2}\, \phi(2^{-m} t - n)$; $n \in Z$ constitutes an unconditional basis for $V_m$.

By property 1, whatever can be seen at a coarse resolution can be seen at a finer resolution. From property 2, in the limits, coarser resolutions see nothing and finer resolutions see everything. Property 3 shows that the spaces of functions can be derived from one another by scaling each approximated function by the ratio of the resolution values. If we require translates of $\phi$ to be an orthonormal basis for $V_0$, then property 4 will be satisfied.

With $P_m$ denoting the orthogonal projection onto $V_m$, we see that $\lim_{m \Rightarrow \infty} P_m f = f$, for all $f \in L^2(R)$. By considering orthogonal projections from $V_{m-1}$ into $V_m$, we have a unique representation for any $P_{m-1} f$ as $P_{m-1} f = P_m f + Q_m f$. The subspace $V_{m-1}$ can be written as the direct sum of $V_m$ and $W_m$ where $V_m = W_m \perp$ and $W_m = V_m \perp$. Also, the orthogonal complements $W_m$ are mutually orthogonal, $W_m \perp W_n$. This means that the collection of mutually orthogonal subspaces partition $L^2(R)$. That is, for $f \in L^2(R)$, we can write $f = \Sigma f_m$, with $\| f \|^2 = \Sigma \| f_m \|^2$, where each $f_m \in W_m$ for each $m \in Z$. For each $m \in Z$, an orthonormal basis $\{\psi_{m,n}\}$ for $W_m$ is the collection of wavelets, and the total collection over m will then be an orthonormal basis for $L^2(R)$.

The use of multi-resolution analysis to develop the concept of wavelets will allow us to generate wavelets based on a construction of a discrete filter. This will be a graphical construction of the wavelets. This summarizes work presented by Mallat [8,9] and Daubechies [4,5]. The filter H, which relates to the function $\Phi$ through the equation, $\Phi(2f) = H(f)\, \Phi(f)$, is the Fourier transform of the sequence $\{h(n)\}$. This means $H(f) = \Sigma\, h(n) \exp(-2\pi i f n)$. We control the $\{h(n)\}$ sequence to build the desired wavelets. These wavelets will have compact support and will form an

orthonormal basis for $L^2(R)$. We place the following conditions on the sequence $\{h(n)\}$:

1) $\Sigma\, |h(n)|\, |n|^{\varepsilon} < \infty$ for some $\varepsilon > 0$ (Regularity)

2) $\Sigma\, h(n-2k)\, h(n-2l) = \delta_{kl}$ (Orthogonality)

3) $\Sigma\, h(n) = 2^{1/2}$ (Normalization)

4) $k_0(z) = \Sigma\, h(n) \exp(inz)$ can be written as

$k_0(z) = 2^{-1} (1 + \exp(iz))^n (\Sigma\, f(n) \exp(inz))$

where $\Sigma\, |f(n)|\, |n|^{\varepsilon} < \infty$ for some $\varepsilon > 0$ and

$\sup_{z \varepsilon R} |\Sigma\, f(n) \exp(inz)| < 2^{N-1}$.

Define $g(n) = (-1)^n h(-n + 1)$, $\phi(z) = (2\pi)^{-1/2} \Pi\, k_0(2^{-j} z)$, $\psi(x) = 2^{1/2} \Sigma\, g(n)\, \phi(2x-n)$, then the $\phi_{j,k}(x) = 2^{-j/2}\, \phi(2^{-j} x - k)$ define a multi-resolution analysis, and the $\psi_{j,k}$ are the associated orthonormal wavelet basis (Daubechies [4,5]). This gives us a means of forming the wavelets by a recursive construction rather than doing an inverse Fourier transform on an infinite product. We use the following functions:

$x_0(t) = \chi_{[-1/2,\, 1/2)}(t)$, indicator function over $[-1/2, 1/2)$

$x_j(t) = 2^{1/2} \Sigma\, h(n)\, x_{j-1}(2t - n)$

$\phi(t) = \lim_{j \Rightarrow \infty} x_j^{(t)}$

$g(n) = (-1)^n h(-n + 1)$

$\psi(t) = 2^{-1/2} \Sigma\, g(n)\, \phi(2t - n)$.

To summarize this process, once the sequence $\{h(n)\}$ has been developed which satisfies the conditions above, the functions $\phi$, g, and $\psi$ are built up recursively from h(n) and $x_j$. In this way, wavelets can be constructed which have compact support and will yield an orthonormal basis for $L^2(R)$. These filters h and g behave as conjugate mirror filters (Smith and Barnwell [11]).

The approximation at each resolution level is computed using a recursive approach which is computationally very efficient and allows for rapid determination of the wavelet coefficients in each resolution level. This process was presented by Mallat [8,9] and Strang [12], and is briefly described as using a pyramid algorithm to form the approximations at each resolution level. The original signal is decomposed into a sum of a coarse resolution term and a collection of detailed

signal terms, the latter being the wavelet decomposition at the finer and finer resolutions. The reconstruction of the signal from the decomposition is also easily computed by reversing the pyramid algorithm process. So, this process allows for efficient decomposition and reconstruction of signals.

## 2.2 Wavelet Filter Formation

The formation of the filter coefficients $\{h_n\}$ which have the desirable properties presented by Daubechies [4,5] can be accomplished through a sequence of algebraic computations. This procedure was also presented by Chui [3]. The set of coefficients $\{h_n\}$ we seek will satisfy the requirements for producing the multi-resolution analysis described in Section 2.1.2. The steps for computing these coefficients for the Daubechies filters are:

1) Select N where 2N is the number of coefficients in the filter, i.e., $\{h_0, h_1, ..., h_{2N-1}\}$

2) Form the trigonometric polynomial

$A(w) = P(\sin(w/2)) = \Sigma_{j=0, ..., N-1} C(N+j,j) (\sin(w/2))^{2j}$

where $C(N,M) = (N!)/((N-M)!)(M!))$

3) Express this polynomial as a function of $\{1, \cos w, ..., \cos Nw\}$, i.e.,

$A(w) = (K_0/2) + \Sigma_{j=1, ..., N} K_j \cos(jw)$

4) Form a polynomial using the coefficients $\{K_j\}$,

$P_A(z) = 2^{-1} \Sigma_{j=-N, ..., N} K_{|j|} z^{N+j}$

5) Solve the equation $P_A(z) = 0$ for the roots, complex $\{z_1, ..., z_J\}$ and real $\{r_1, ..., r_L\}$. The complex roots come in quadruplets, $z_j$, $\bar{z}_j$, $z_{j-1}$, $\bar{z}_{j-1}$. The real roots come in pairs, $r_l$, $r_l^{-1}$.

6) Select one complex root $z_j$ from each quadruplet and one real root $r_l$ from each pair, with $|z_j| > 1$ and $|r_l| > 1$.

7) Form the polynomial $B(z) = \Pi (z - z_j) \Pi (z - r_l)$.

8) Form $S(z) = -B(z)/B(1)$ where $B(1)$ is $B(z)$ when $z = 1$.

9) Form $P(z) = ((1 + z)/2)^{N+1} \cdot S(z) \cdot 2^{1/2} = \Sigma_{k=0, ..., 2N-1} p_k z^k$

10) The coefficients of P(z), $\{p_n\}$, are the filter coefficients $\{h_n\}$, i.e., $h_n = p_n$.

This procedure is illustrated as follows:

1) Let N = 2, which will yield the Daubechies filter with 4 coefficients $\{h_0, h_1, h_2, h_3\}$

2) Form the A(w) polynomial,

$A(w) = \Sigma_{j=0,1} C(1+j,j) (\sin (w/2))^{2j}$

$A(w) = 2 - \cos (w)$

3) Next we form $P_A(z) = 2^{-1} [-1 + 4z - z^2]$

4) Find the roots of $P_A(z) = 0$. This has roots $2 \pm 3^{1/2}$ with the plus root outside the unit circle

5) Form the polynomial $B(z) = \Pi (z - z_j) \Pi (z - r_l)$

6) Compute the function $S(z) = -B(z)/B(1)$,

$S(z) = (-2)^{-1} ((3^{1/2} - 1) z - (3^{1/2} + 1))$

7) Form the polynomial $P(z) = ((1+z)/2)^{N+1} \cdot S(z) \cdot 2^{1/2}$

$P(z) = (1/(4 \cdot 2^{1/2}) ((1+3^{1/2}) + (3+3^{1/2}) z + (3-3^{1/2}) z^2 + (1-3^{1/2}) z^3)$

8) Finally, the four coefficients for the Daubechies filter are given by the coefficients of this polynomial P(z), i.e.,

$h_0 = (1/(4 \cdot 2^{1/2}) (1+3^{1/2})$

$h_1 = (1/(4 \cdot 2^{1/2}) (3+3^{1/2})$

$h_2 = (1/(4 \cdot 2^{1/2}) (3-3^{1/2})$

$h_3 = (1/(4 \cdot 2^{1/2}) (1-3^{1/2})$.

## 2.3 Wavelet Decomposition and Reconstruction

Use of wavelets to transform the original data vector into a collection of wavelet coefficients may be interpreted in several ways. Two that we used are described in this section. Also, the collection of wavelet coefficients that may be computed will vary depending on the length of the original signal vector. For example, if the vector has length 8, then there are 3 levels possible, and each level will involve 8 terms for a total of 24. Instead, if the original signal has 16

terms, then 4 levels are possible and 64 terms may be generated. Table 3 shows the various levels and the different terms which can be created. We use the symbol 's' to indicate that a sum or an averaging was computed and 'd' to indicate that a difference was computed. This relates to the scaling function and the wavelet function by associating sums with the scaling function $\phi$ and differences with the wavelet function $\psi$. To understand this table for a particular item, say dsds, which is ordered from right to left, we mean that first a sum is computed, then a difference, then a sum and finally a difference. We observe that to form an orthonormal basis, we only need pick a collection of terms which cover the chart horizontally and do not overlap vertically. For example, the terms ssss, dsss, $dss_0$, $dss_1$, $ds_0$, $ds_1$, $ds_2$, $ds_3$, $d_0$, $d_1$, $d_2$, $d_3$, $d_4$, $d_5$, $d_6$, and $d_7$ would compose an orthonormal basis. Another basis would be the set $\{s_0, s_1, s_2, s_3, s_4, s_5, s_6, s_7, s_0,$ $s_0$, sssd, dssd, sdsd, ddsd, $sdd_0$, $sdd_1$, $ddd_0$, $ddd_1\}$. We see that many potential bases exist. In fact, for a vector of length N, there are $2^{N/2} + 1$ unique potential bases.

**Table 3. Wavelet Coefficients for a Signal of Length 16.**

| | | | | | | | | | | | | | | | |
|---|---|---|---|---|---|---|---|---|---|---|---|---|---|---|---|
| $x_0$ | $x_1$ | $x_2$ | $x_3$ | $x_4$ | $x_5$ | $x_6$ | $x_7$ | $x_8$ | $x_9$ | $x_{10}$ | $x_{11}$ | $x_{12}$ | $x_{13}$ | $x_{14}$ | $x_{15}$ |
| $s_0$ | $s_1$ | $s_2$ | $s_3$ | $s_4$ | $s_5$ | $s_6$ | $s_7$ | $d_0$ | $d_1$ | $d_2$ | $d_3$ | $d_4$ | $d_5$ | $d_6$ | $d_7$ |
| $ss_0$ | $ss_1$ | $ss_2$ | $ss_3$ | $ds_0$ | $ds_1$ | $ds_2$ | $ds_3$ | $sd_0$ | $sd_1$ | $sd_2$ | $sd_3$ | $dd_0$ | $dd_1$ | $dd_2$ | $dd_3$ |
| $sss_0$ | $sss_1$ | $dss_0$ | $dss_1$ | $sds_0$ | $sds_1$ | $dds_0$ | $dds_1$ | $ssd_0$ | $ssd_1$ | $dsd_0$ | $dsd_1$ | $sdd_0$ | $sdd_1$ | $ddd_0$ | $ddd_1$ |
| ssss | dsss | sdss | ddss | ssds | dsds | sdds | ddds | sssd | dssd | sdsd | ddsd | ssdd | dsdd | sddd | dddd |

The collection of coefficients to use when a signal is transformed can be extracted from Table 3. This approach corresponds to the wavelet packets method described by Coifman and Wickerhauser [1,2]. Their technique is based on examining the ability of the decomposition to describe the signal. This is quantified by considering the entropy cost in each decomposition and selecting the decomposition with the minimum cost.

For the second approach, the decomposition of a signal into these coefficients at the different resolution levels is greatly facilitated by employing a convolution operation. We denote

the scaling function filter $\phi$ by a convolution with the filter H and the wavelet filter $\psi$ by a convolution with the filter G. The sequence of steps for reaching the 4 levels described above can be visualized by the operations depicted in Figure 5. An incoming signal of length 16 enters the filter stream. Each of the operators is either a convolution with H or G followed by a decimation into half the number of terms. These modified signals are then operated on at the next step. This continues for 4 iterations. The resulting terms produced are identical to the collection in Table 3. Figure 5 also denotes the various terms being computed at each point using the same s and d notation.

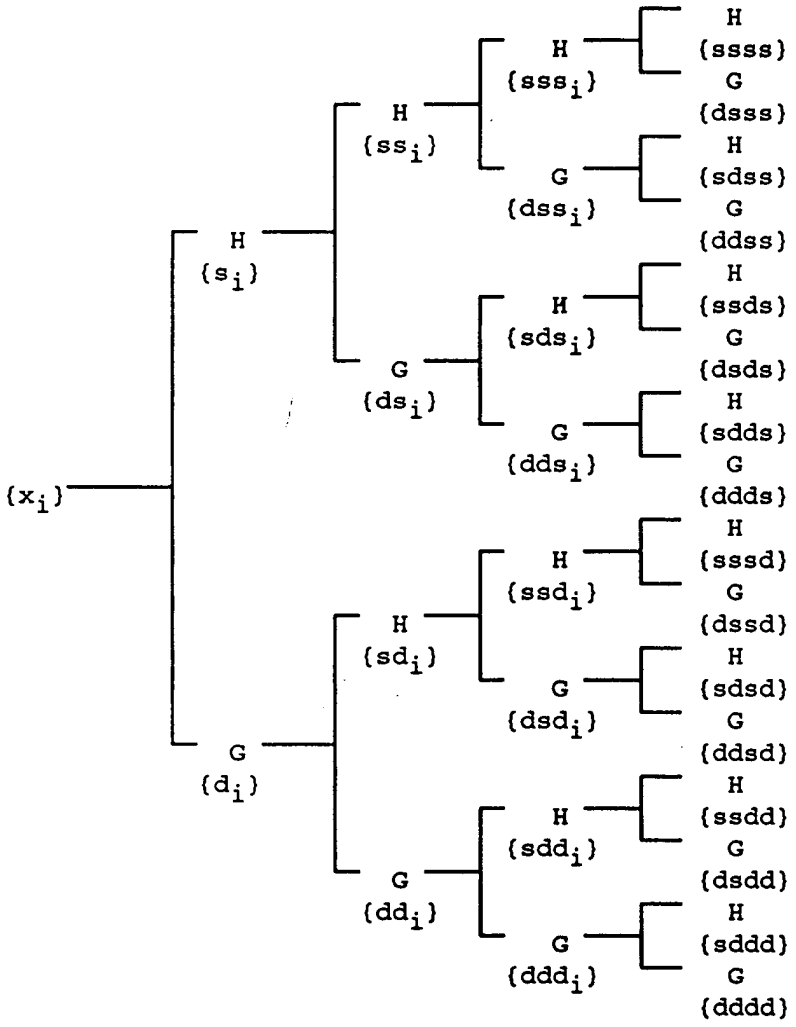


**Figure 5. Wavelet Coefficient Construction from H, G Filters**

Reconstruction of the signal from wavelet coefficients can be achieved by reversing the above steps. This is accomplished by observing that the inverse operators to H and G are their adjoints H* and G*. The adjoints of these operators are their conjugate transposes. By summing the results of these adjoint operators on the coefficients at one level, the coefficients at the preceding level can be recovered. At level one this looks like: $\{x_i\} = H^*(\{s_i\}) + G^*(\{d_i\})$. Since this method can be applied at each of the levels, the original signal can be reconstructed from the various coefficients at the set of levels.

Convolution operators may also be interpreted in terms of a linear transformation of the original signal. By using a matrix to represent the transformation, these convolutions can be replaced with a matrix multiplication. If the signal is not very long, this replacement will not produce a large increase in computations and will simplify the implementation by fixing the computation of each coefficient.

This can be illustrated for two types of filters, the Haar with two coefficients and the Daubechies filter D04 with four coefficients. Figure 6 shows the matrix for the Haar filter. If the incoming signal of length 16 is transformed by this matrix, the resulting vector is the set of wavelet coefficients for the basis {ssss, dsss, $\{dss_i\}$, $\{ds_i\}$, $\{d_i\}$}. For the matrix to be unitary, we need to divide each row by its norm. For example, row 1 needs to be divided by 4. Figure 7 shows the matrix which would represent the Daubechies D04 filter for a signal of length 16. It is broken into the sum of two matrices, with the second having the square root of 3 as a factor.

## 2.4 Time Frequency Localization

Converting a data vector to wavelet-based representation is similar to performing a Fourier transform. However, differences arise in the basis functions used. When the discrete Fourier transform is applied to a data vector, the result is a representation of the vector in the space spanned by complex exponentials. The vector is expressed as a combination of complex exponentials of the

$$W = \begin{bmatrix}
1 & 1 & 1 & 1 & 1 & 1 & 1 & 1 & 1 & 1 & 1 & 1 & 1 & 1 & 1 & 1 \\
1 & 1 & 1 & 1 & 1 & 1 & 1 & 1 & -1 & -1 & -1 & -1 & -1 & -1 & -1 & -1 \\
1 & 1 & 1 & 1 & -1 & -1 & -1 & -1 & 0 & 0 & 0 & 0 & 0 & 0 & 0 & 0 \\
0 & 0 & 0 & 0 & 0 & 0 & 0 & 0 & 1 & 1 & 1 & 1 & -1 & -1 & -1 & -1 \\
1 & 1 & -1 & -1 & 0 & 0 & 0 & 0 & 0 & 0 & 0 & 0 & 0 & 0 & 0 & 0 \\
0 & 0 & 0 & 0 & 1 & 1 & -1 & -1 & 0 & 0 & 0 & 0 & 0 & 0 & 0 & 0 \\
0 & 0 & 0 & 0 & 0 & 0 & 0 & 0 & 1 & 1 & -1 & -1 & 0 & 0 & 0 & 0 \\
0 & 0 & 0 & 0 & 0 & 0 & 0 & 0 & 0 & 0 & 0 & 0 & 1 & 1 & -1 & -1 \\
1 & -1 & 0 & 0 & 0 & 0 & 0 & 0 & 0 & 0 & 0 & 0 & 0 & 0 & 0 & 0 \\
0 & 0 & 1 & -1 & 0 & 0 & 0 & 0 & 0 & 0 & 0 & 0 & 0 & 0 & 0 & 0 \\
0 & 0 & 0 & 0 & 1 & -1 & 0 & 0 & 0 & 0 & 0 & 0 & 0 & 0 & 0 & 0 \\
0 & 0 & 0 & 0 & 0 & 0 & 1 & -1 & 0 & 0 & 0 & 0 & 0 & 0 & 0 & 0 \\
0 & 0 & 0 & 0 & 0 & 0 & 0 & 0 & 1 & -1 & 0 & 0 & 0 & 0 & 0 & 0 \\
0 & 0 & 0 & 0 & 0 & 0 & 0 & 0 & 0 & 0 & 1 & -1 & 0 & 0 & 0 & 0 \\
0 & 0 & 0 & 0 & 0 & 0 & 0 & 0 & 0 & 0 & 0 & 0 & 1 & -1 & 0 & 0 \\
0 & 0 & 0 & 0 & 0 & 0 & 0 & 0 & 0 & 0 & 0 & 0 & 0 & 0 & 1 & -1
\end{bmatrix}$$

**Figure 6. Haar Transform Matrix**

form, exp (-int). When wavelets are used, a set of wavelet basis functions is used to span the signal space. A signal is represented in the wavelet space in terms of linear combinations of wavelets rather than complex exponentials, as was done with the Fourier transform.

An analogy with written music composed of a scale and notes helps to illustrate a major difference between using Fourier coefficients and wavelet coefficients to represent a signal. The location of the note on the scale tells when the note is to occur, what frequency it will have, and its duration. When a signal is written in its Fourier coefficient form, its frequency content is being highlighted by the magnitude of the coefficient associated with each particular frequency.

However, when a frequency occurs in time, its time localization is not available in the ordinary Fourier transform. With wavelets, both frequency information and time localization information are presented. This makes the wavelet description similar to written music score, with its time and frequency information being depicted simultaneously. By making a judicious choice of wavelet basis functions, the data vector may be adequately represented with fewer terms.

This capacity to localize in time and frequency with wavelets comes from the manner in which the wavelet basis is constructed. Since the various functions are produced by dilations and shifts of the generating wavelet, the location of frequency content can be readily found. Fourier

$$W = \begin{bmatrix}
4 & 4 & 4 & 4 & 4 & 4 & 4 & 4 & 4 & 4 & 4 & 4 & 4 & 4 & 4 & 4 \\
4 & 8 & 10 & 10 & 8 & 4 & -2 & 2 & -4 & -8 & -10 & -10 & -8 & -4 & 2 & -2 \\
24 & 16 & -12 & 12 & -16 & -24 & -12 & -28 & -8 & 0 & -4 & 4 & 0 & 8 & 28 & 12 \\
-8 & 0 & -4 & 4 & 0 & 8 & 28 & 12 & 24 & 16 & -12 & 12 & -16 & -24 & -12 & -28 \\
-6 & 6 & 2 & -6 & 0 & 2 & 0 & 0 & 0 & 0 & 0 & 0 & -2 & 0 & 6 & -2 \\
-2 & 0 & 6 & -2 & -6 & 6 & 2 & -6 & 0 & 2 & 0 & 0 & 0 & 0 & 0 & 0 \\
0 & 0 & 0 & 0 & -2 & 0 & 6 & -2 & -6 & 6 & 2 & -6 & 0 & 2 & 0 & 0 \\
0 & 2 & 0 & 0 & 0 & 0 & 0 & 0 & -2 & 0 & 6 & -2 & -6 & 6 & 2 & -6 \\
3 & -1 & 0 & 0 & 0 & 0 & 0 & 0 & 0 & 0 & 0 & 0 & 0 & 0 & 1 & -3 \\
1 & -3 & 3 & -1 & 0 & 0 & 0 & 0 & 0 & 0 & 0 & 0 & 0 & 0 & 0 & 0 \\
0 & 0 & 1 & -3 & 3 & -1 & 0 & 0 & 0 & 0 & 0 & 0 & 0 & 0 & 0 & 0 \\
0 & 0 & 0 & 0 & 1 & -3 & 3 & -1 & 0 & 0 & 0 & 0 & 0 & 0 & 0 & 0 \\
0 & 0 & 0 & 0 & 0 & 0 & 1 & -3 & 3 & -1 & 0 & 0 & 0 & 0 & 0 & 0 \\
0 & 0 & 0 & 0 & 0 & 0 & 0 & 0 & 1 & -3 & 3 & -1 & 0 & 0 & 0 & 0 \\
0 & 0 & 0 & 0 & 0 & 0 & 0 & 0 & 0 & 0 & 1 & -3 & 3 & -1 & 0 & 0 \\
0 & 0 & 0 & 0 & 0 & 0 & 0 & 0 & 0 & 0 & 0 & 0 & 1 & -3 & 3 & -1
\end{bmatrix}$$

$$+ \sqrt{3} \begin{bmatrix}
0 & 0 & 0 & 0 & 0 & 0 & 0 & 0 & 0 & 0 & 0 & 0 & 0 & 0 & 0 & 0 \\
-8 & -4 & -2 & 2 & 4 & 8 & 14 & 14 & 8 & 4 & 2 & -2 & -4 & -8 & -14 & -14 \\
0 & 24 & 52 & 52 & 24 & 0 & -20 & -28 & -16 & -8 & -4 & -4 & -8 & -16 & -28 & -20 \\
-16 & -8 & -4 & -4 & -8 & -16 & -28 & -20 & 0 & 24 & 52 & 52 & 24 & 0 & -20 & -28 \\
10 & 10 & -2 & -6 & -2 & 0 & 0 & 0 & 0 & 0 & 0 & 0 & 0 & -2 & -6 & -2 \\
0 & -2 & -6 & -2 & 10 & 10 & -2 & -6 & -2 & 0 & 0 & 0 & 0 & 0 & 0 & 0 \\
0 & 0 & 0 & 0 & 0 & -2 & -6 & -2 & 10 & 10 & -2 & -6 & -2 & 0 & 0 & 0 \\
-2 & 0 & 0 & 0 & 0 & 0 & 0 & 0 & 0 & -2 & -6 & -2 & 10 & 10 & -2 & -6 \\
1 & -1 & 0 & 0 & 0 & 0 & 0 & 0 & 0 & 0 & 0 & 0 & 0 & 0 & -1 & 1 \\
-1 & 1 & 1 & -1 & 0 & 0 & 0 & 0 & 0 & 0 & 0 & 0 & 0 & 0 & 0 & 0 \\
0 & 0 & -1 & 1 & 1 & -1 & 0 & 0 & 0 & 0 & 0 & 0 & 0 & 0 & 0 & 0 \\
0 & 0 & 0 & 0 & -1 & 1 & 1 & -1 & 0 & 0 & 0 & 0 & 0 & 0 & 0 & 0 \\
0 & 0 & 0 & 0 & 0 & 0 & -1 & 1 & 1 & -1 & 0 & 0 & 0 & 0 & 0 & 0 \\
0 & 0 & 0 & 0 & 0 & 0 & 0 & 0 & -1 & 1 & 1 & -1 & 0 & 0 & 0 & 0 \\
0 & 0 & 0 & 0 & 0 & 0 & 0 & 0 & 0 & 0 & -1 & 1 & 1 & -1 & 0 & 0 \\
0 & 0 & 0 & 0 & 0 & 0 & 0 & 0 & 0 & 0 & 0 & 0 & -1 & 1 & 1 & -1
\end{bmatrix}$$

**Figure 7. Daubechies D04 Transform Matrix**

transforms that are windowed, such as the Gabor transform (Gabor [7]), provide some time frequency localization. However, wavelets maintain an advantage in that for low frequency occurrences in the signal, the wavelet with a long dilation and hence a low frequency matches up with the signal. On the other hand, for high frequency occurrences, the wavelet with a short dilation and hence a high frequency matches up with the signal. It is this property of wavelets that makes them match up with the signal in fewer terms and therefore provides efficient time frequency localization.

Analyzing signals with wavelets may be described with the use of time frequency plots. The time frequency plot describes the frequency content of the signal and its time location within the uncertainty limits. Figures 8 through 11 show these plots for various choices of signals and wavelet bases. For these plots, the signal to be analyzed is shown along the bottom. The easiest signal to discuss is the spike shown in Figure 8, in which the spike has very short time duration. The spike is given in the lower plot, while its time frequency plot is shown above. This plot shows a strong localization in time for this signal and a large spread in frequency, which is clearly the correct interpretation for this spike signal. It is of interest to remember that the Fourier Transform of a dirac delta function is an infinite frequency spectrum.

Figure 9 shows a signal with varying intensity magnitude and covering a longer period of time. Its time frequency plot depicts this by starting with lighter (weaker) rectangles and increasing in darkness as the intensity increases. Also, the spread of frequencies covers the full range. The signal shown in Figure 10 starts with a high intensity pulse and dampens out over time. This is shown in the time frequency plot by having the rectangles begin appearing at the time of the pulse and the intensities of these rectangles decrease over time, indicating a weaker and weaker intensity signal. Figure 11 shows a signal with various intensities and frequencies over the time interval. The time frequency plot shows this assorted collection by various rectangles and intensities over the interval. Occasional higher frequencies appear, but mainly lower frequency rectangles dominate. These time frequency plots show the interplay between time and frequency for a

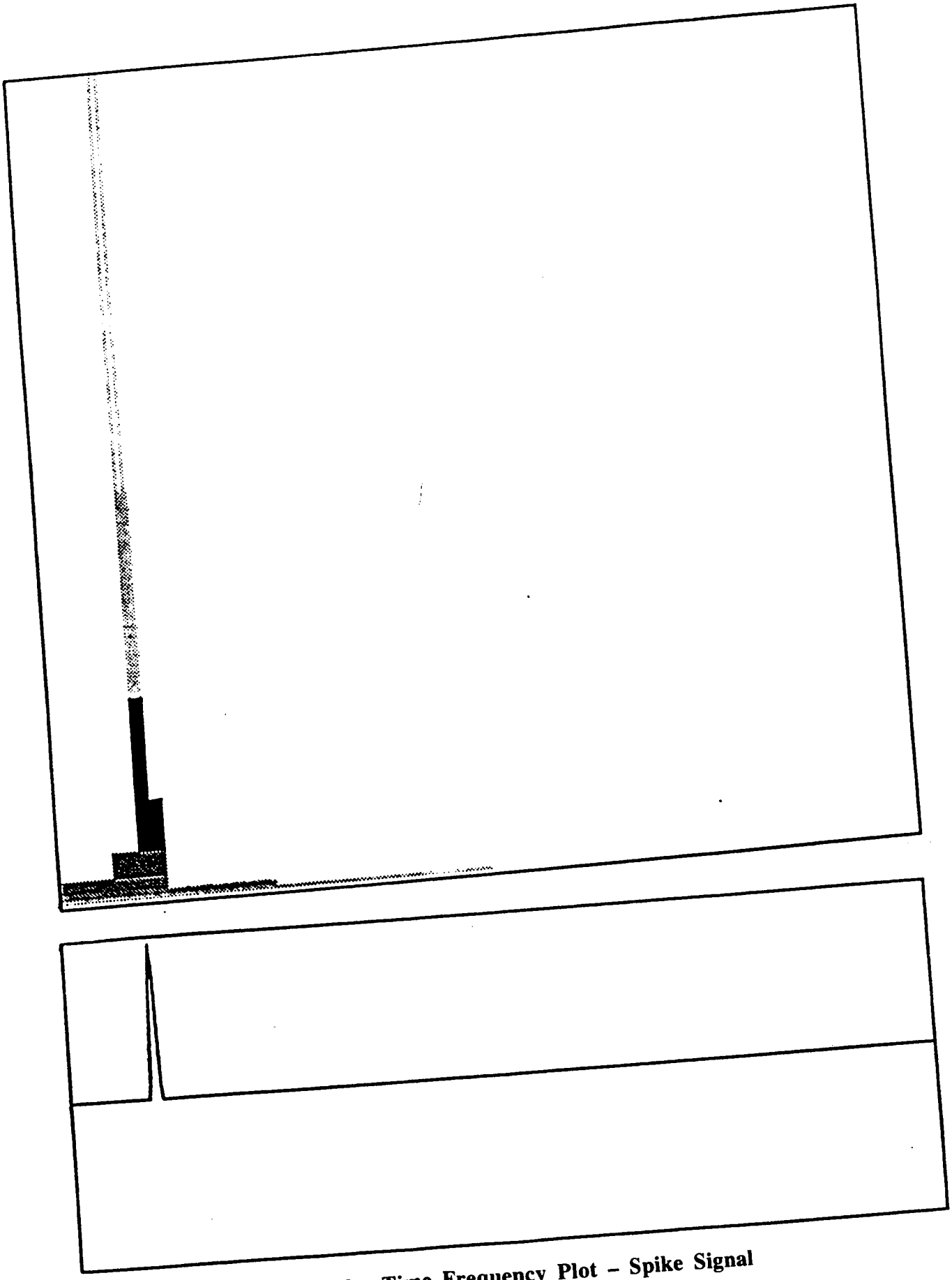

**Figure 8. Time Frequency Plot – Spike Signal**

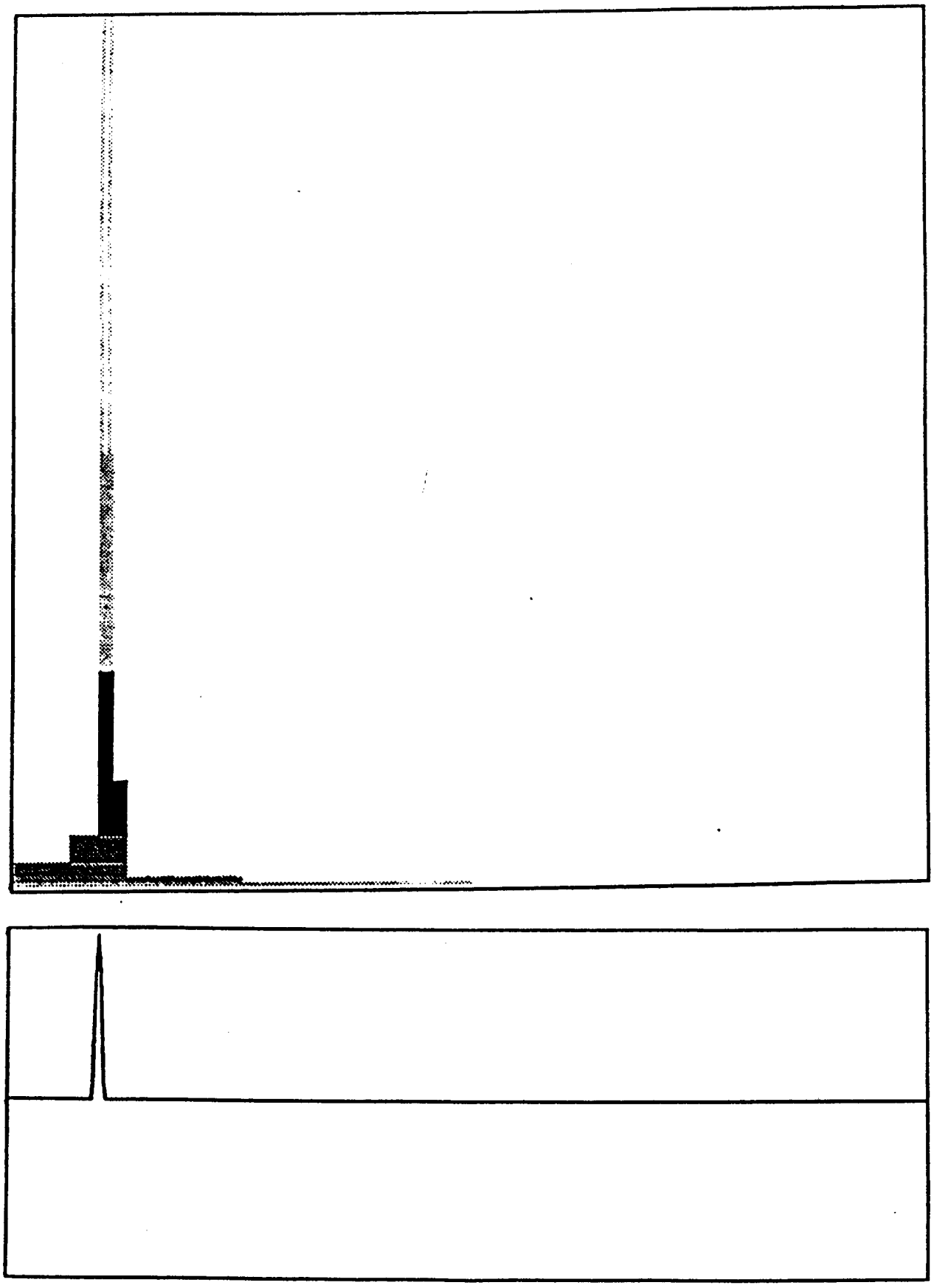

**Figure 8. Time Frequency Plot – Spike Signal**

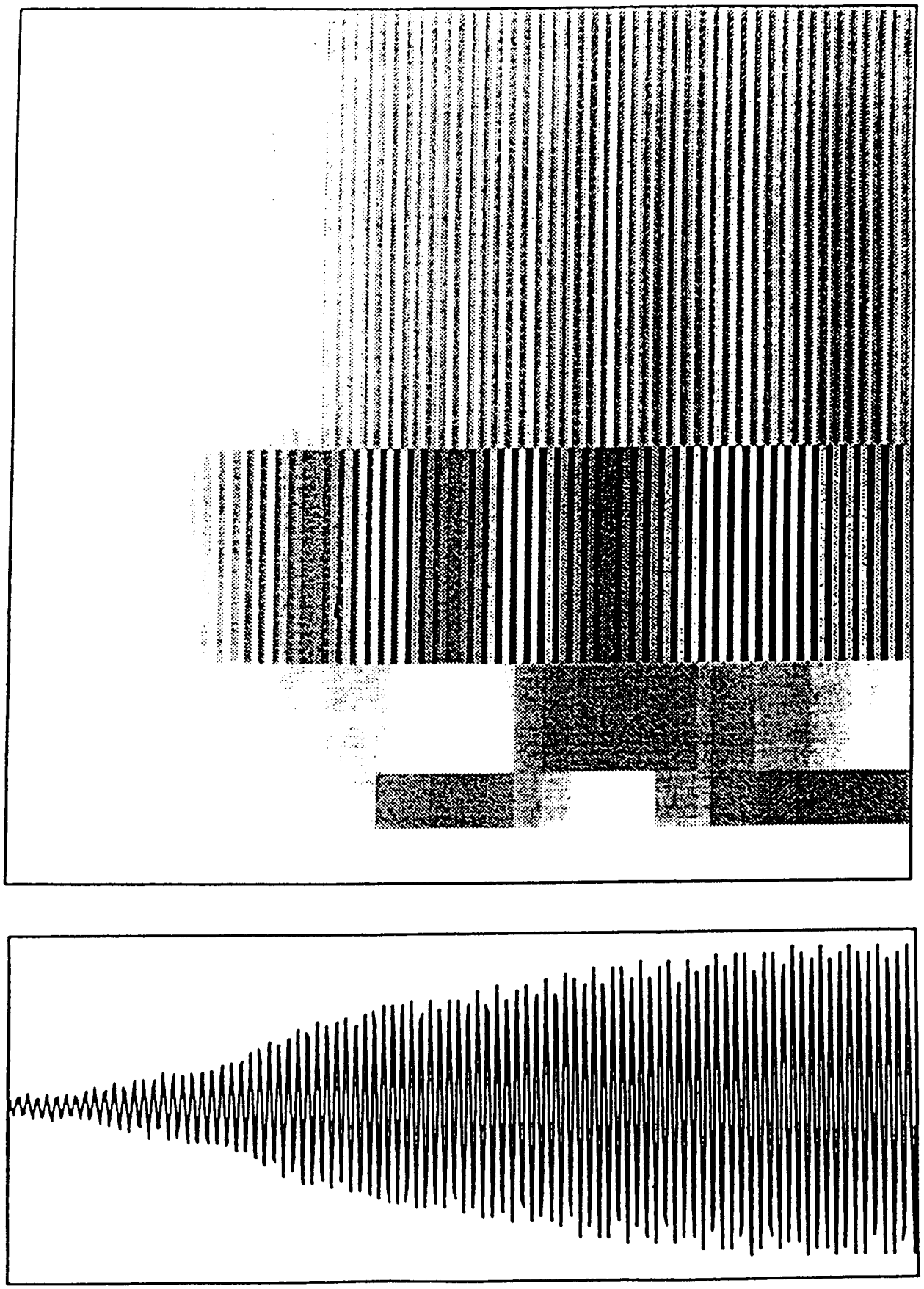

**Figure 9. Time Frequency Plot – Varying Intensity Signal**

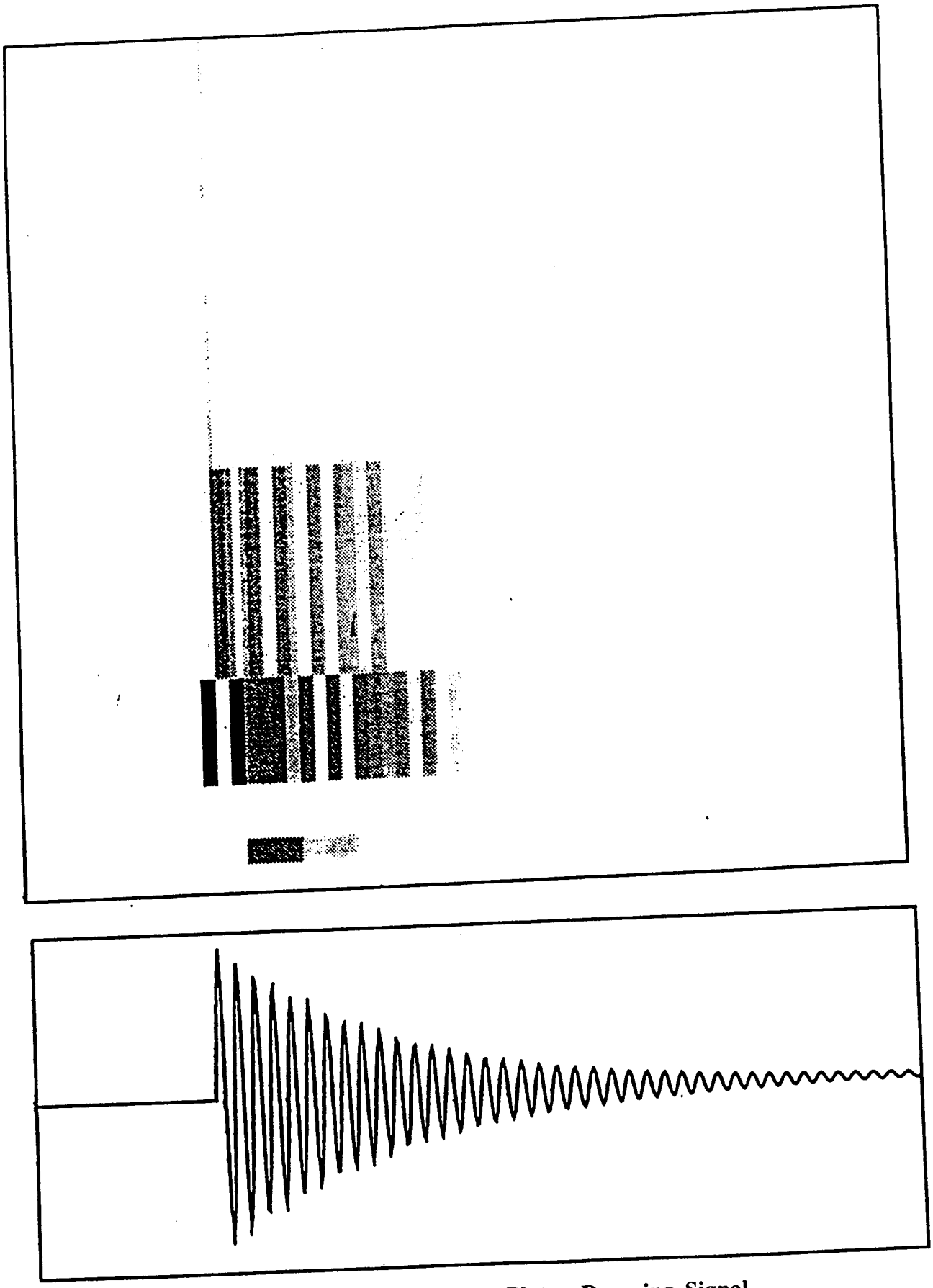

**Figure 10. Time Frequency Plot – Damping Signal**

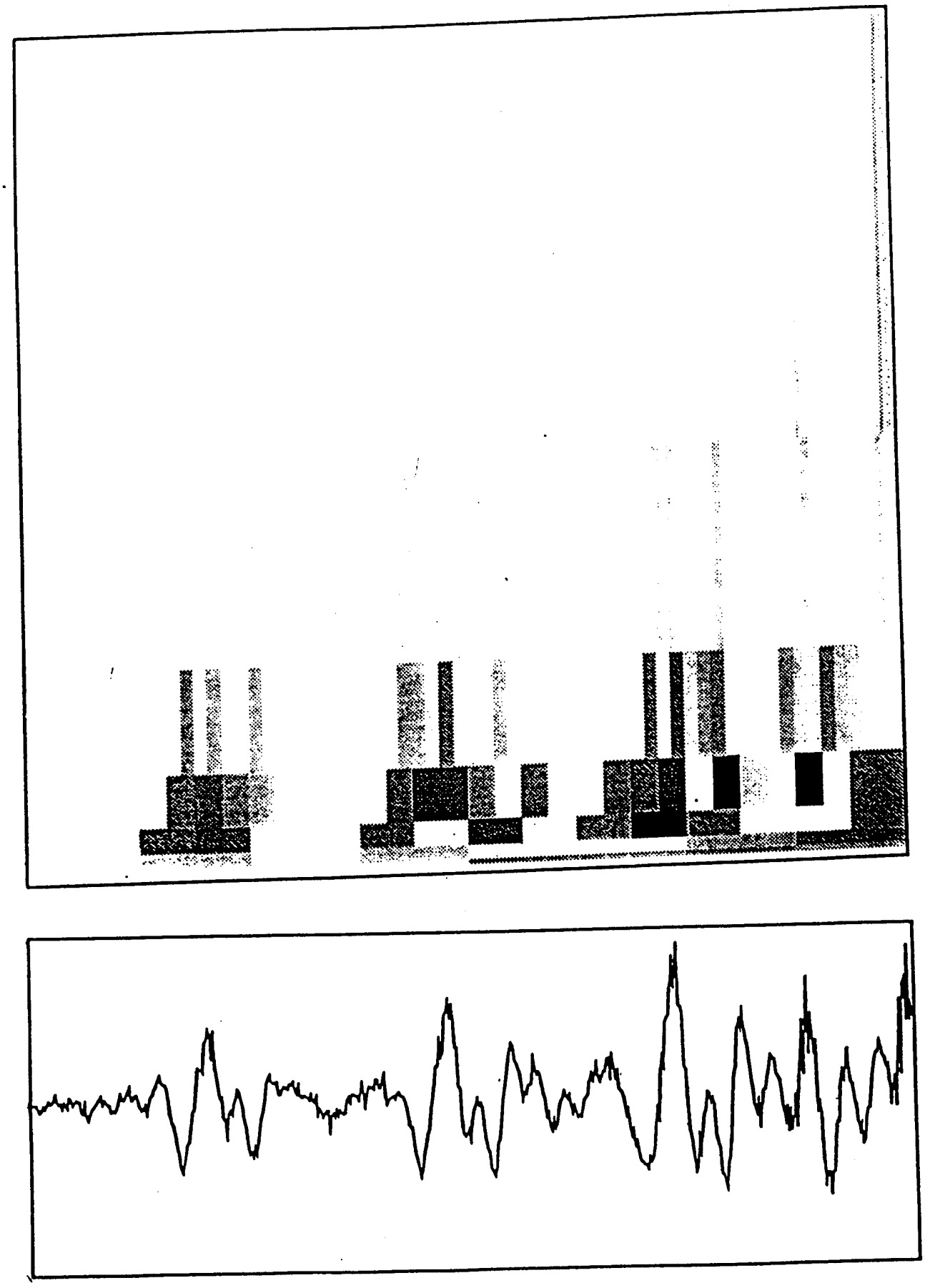

**Figure 11. Time Frequency Plot – Varying Frequency Signal**

particular signal. This relates to depicting the intensity of the coefficients for the wavelet bases over the various choices of frequency level (or resolution level). So, these plots show how a signal is decomposed into its various resolution levels.

Time frequency plots were applied to radar HRRPs for various target samples as shown in Figures 12 through 17. In this case, the input signal is the HRRP for the sample shown at the bottom. The time frequency plots show the intensity of the wavelet coefficients for various resolution levels. The plots indicate that the number of rectangles needed to describe the signal is approximately eight, which is about half of the number of data points input to the wavelet decomposition. This indicates that reduction in the number of features should behave favorably in terms of classifier performance and should not affect classifier performance with a two-to-one reduction in features. This supports the anticipated reduction in dimensionality of the feature space.

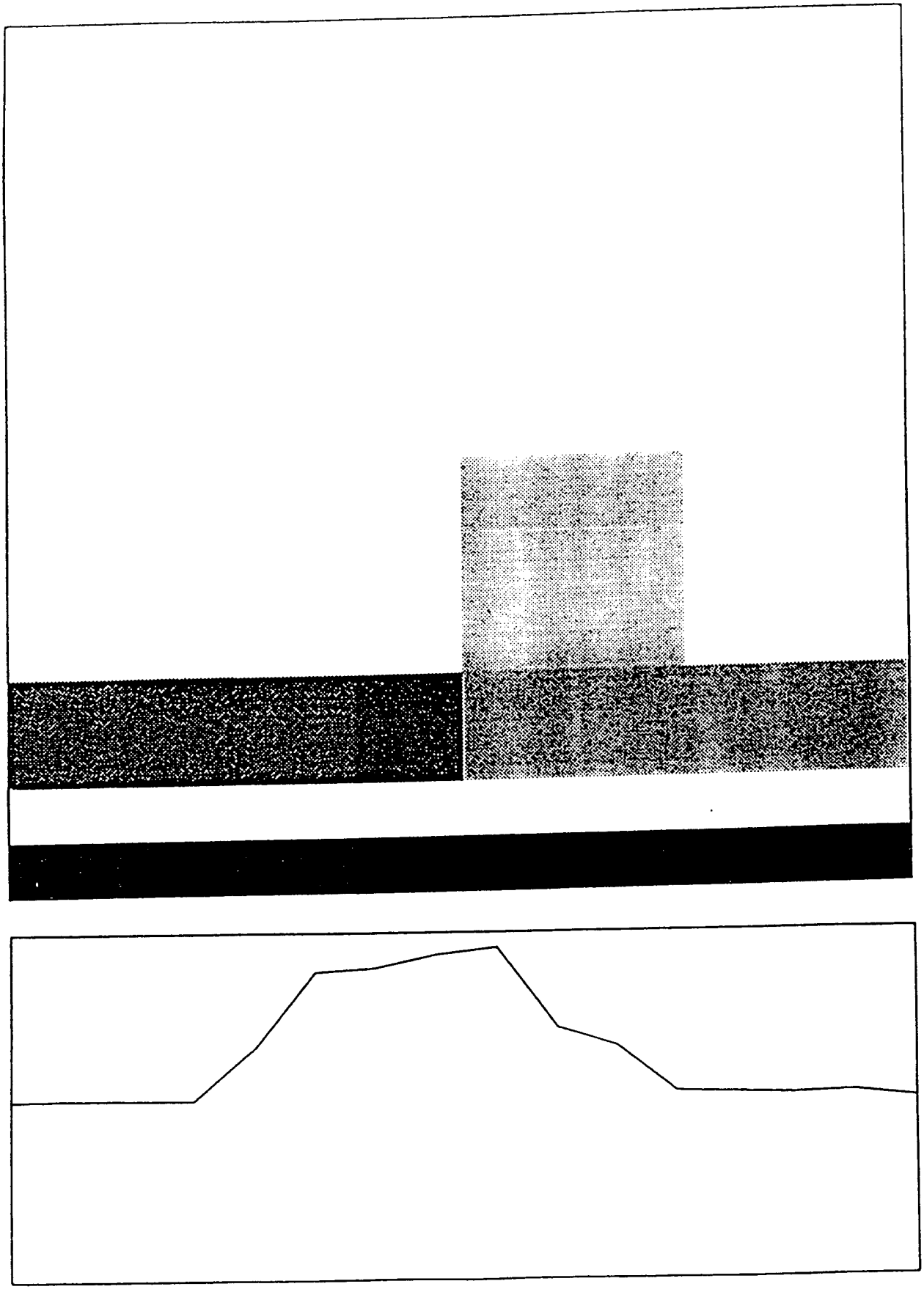

**Figure 12. Time Frequency Plot – HRRP Sample 1**

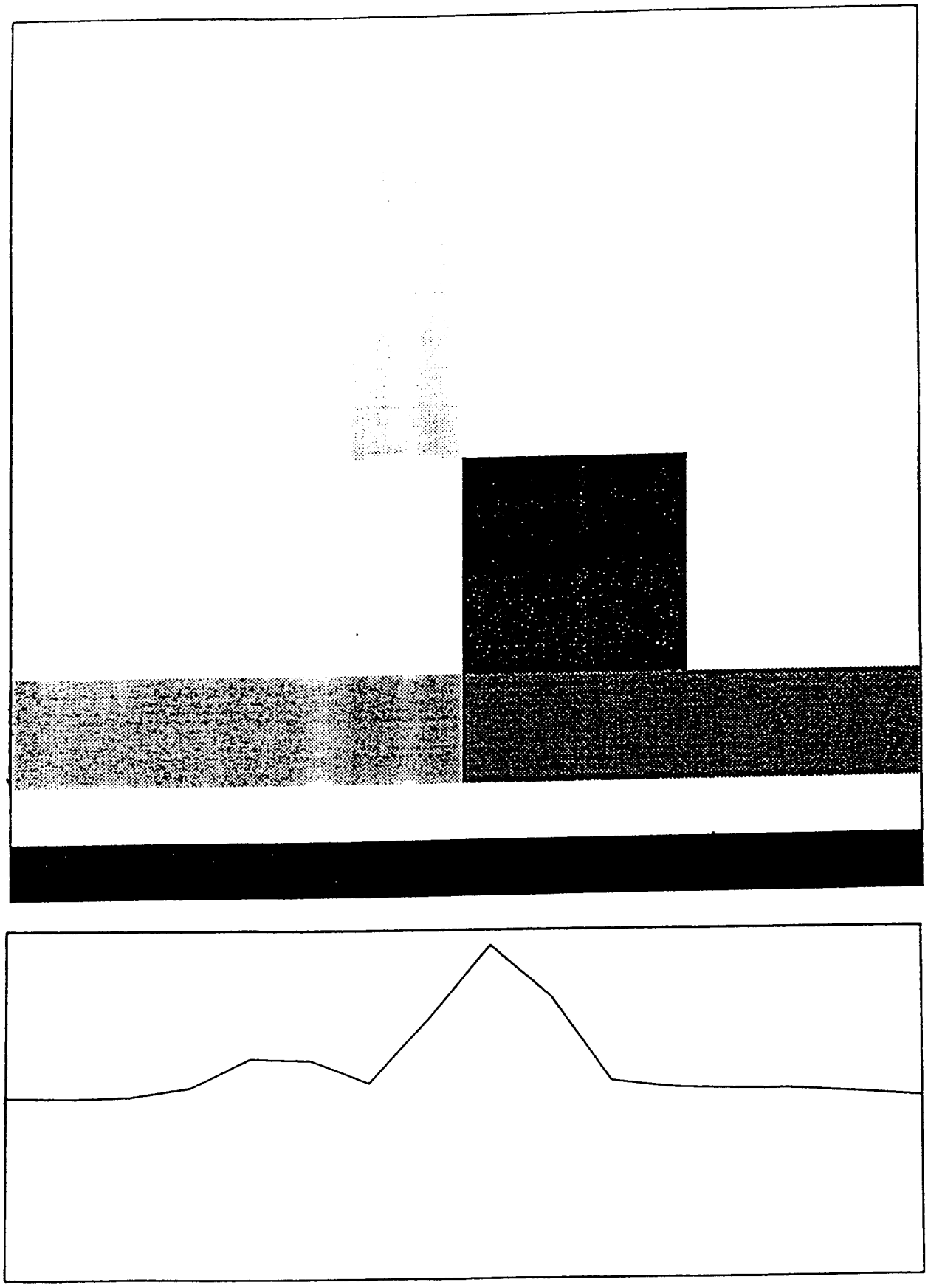

**Figure 13. Time Frequency Plot – HRRP Sample 2**

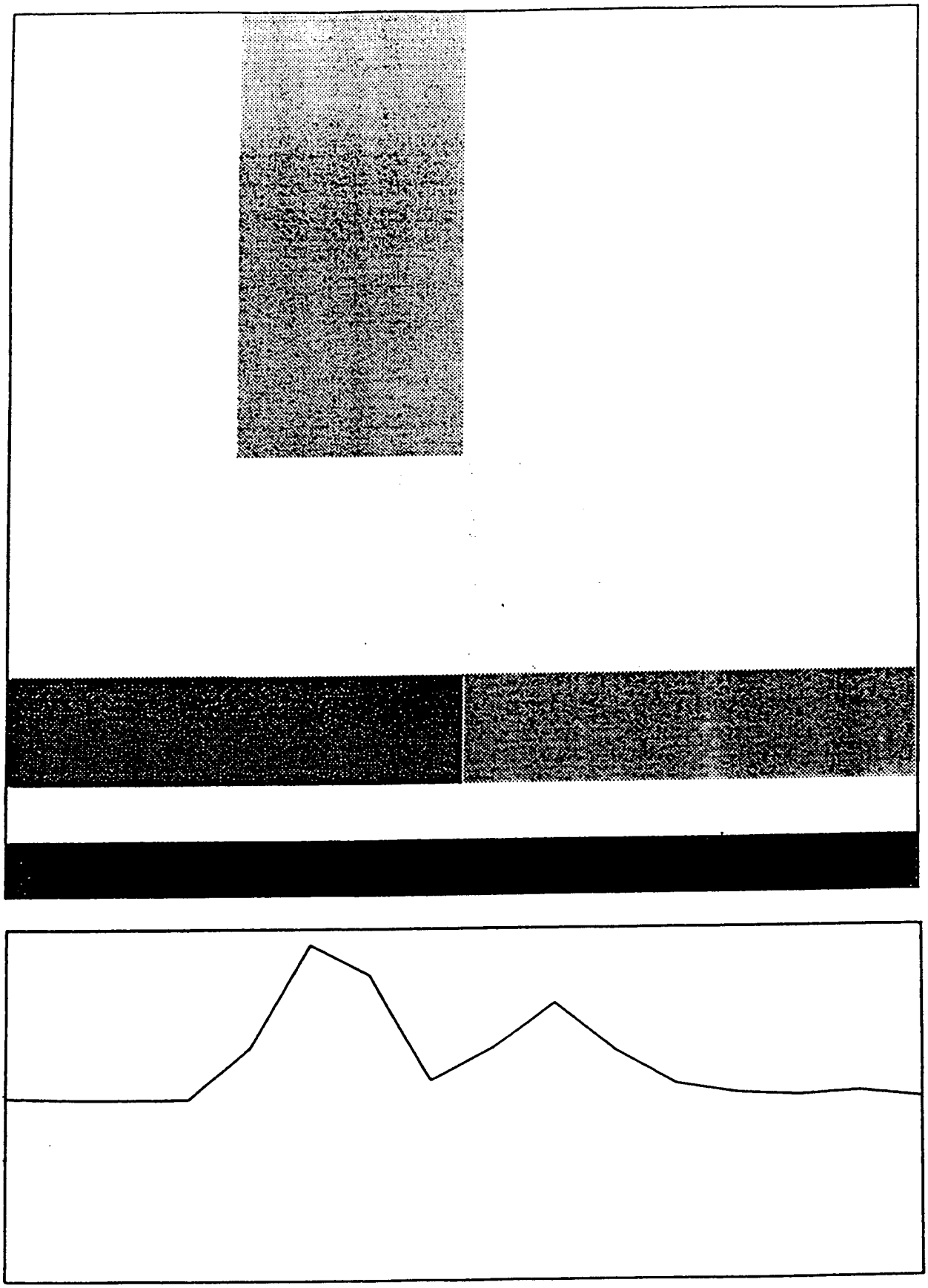

**Figure 14. Time Frequency Plot – HRRP Sample 3**

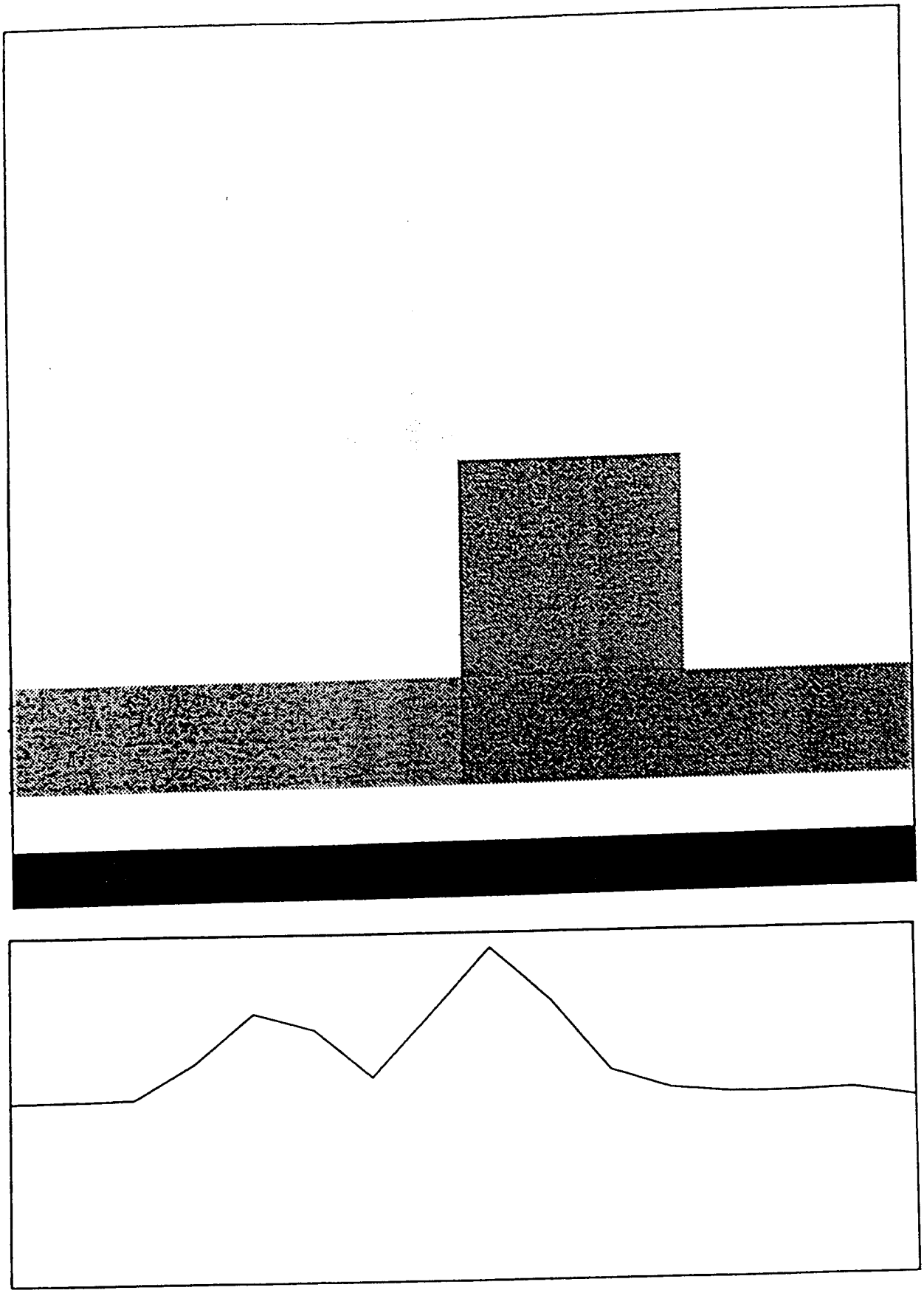

**Figure 15. Time Frequency Plot – HRRP Sample 4**

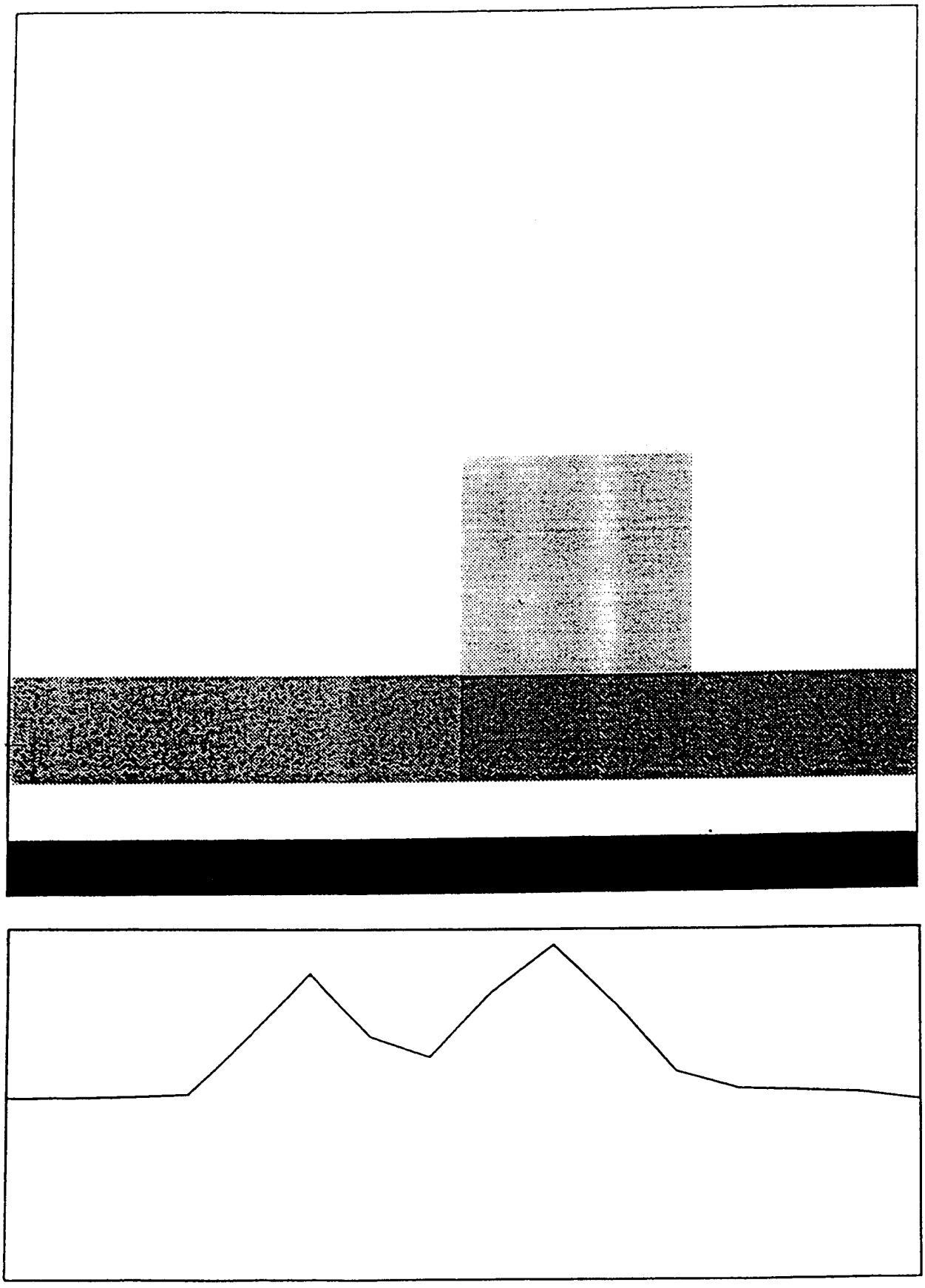

**Figure 16. Time Frequency Plot – HRRP Sample 5**

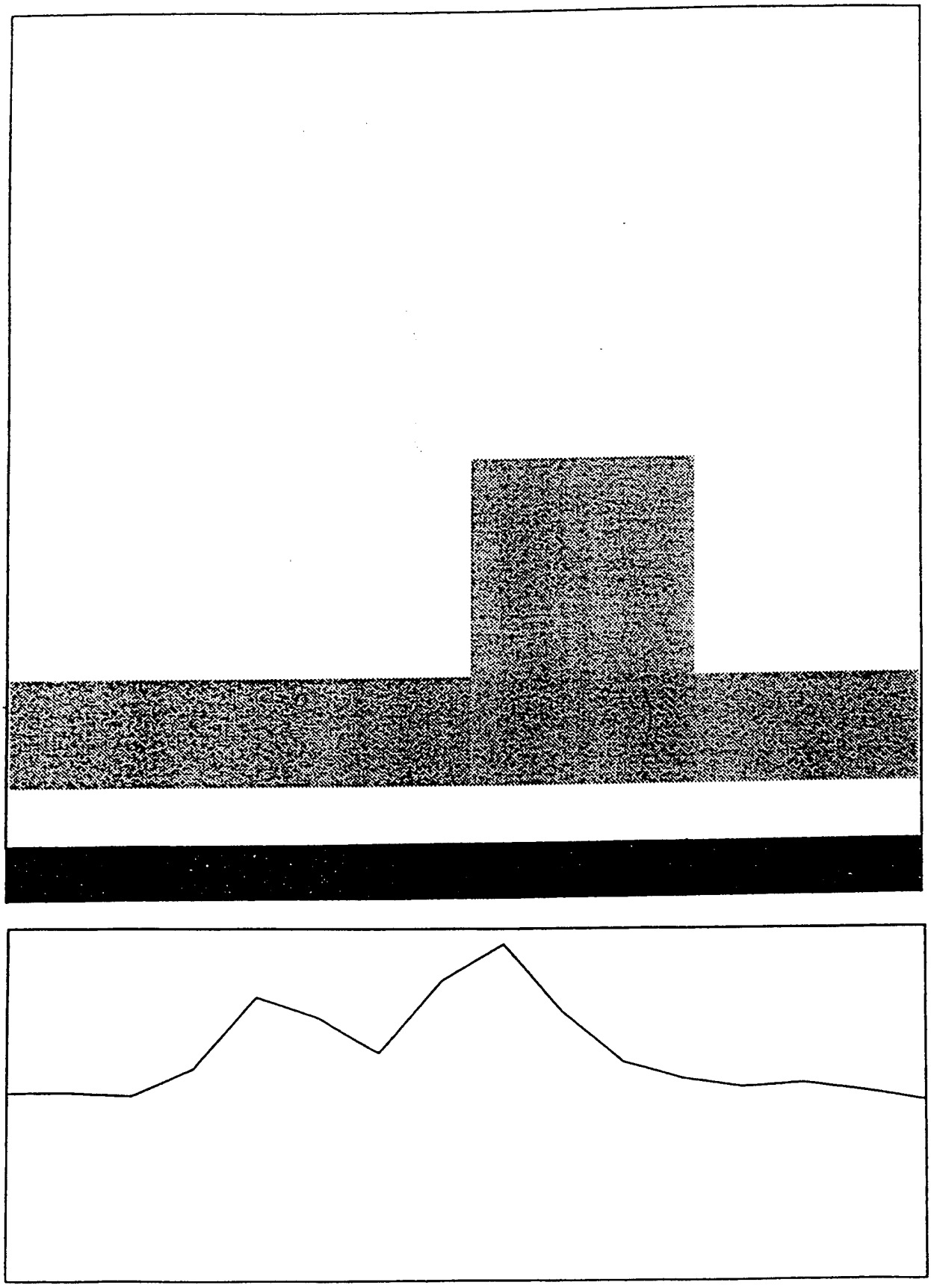

**Figure 17. Time Frequency Plot – HRRP Sample 6**

## 3.0 FEATURE EXTRACTION AND CLASSIFICATION

Wavelets can be used to replace the ordinary feature set as a modified feature extraction process. This is depicted in Figure 18. The wavelet coefficients are processed rather than the original features. This may be beneficial in different ways. First, it reduces the number of features while maintaining the performance level. Second, it can lead to more effective features. Third, it could also provide a more robust set of features, since it involves an averaging process. It has already been discussed that many choices exist for wavelet bases once a particular wavelet has been selected. By varying the choice of wavelet and the choice of wavelet basis, many different sets of features can be constructed for one set of input data.

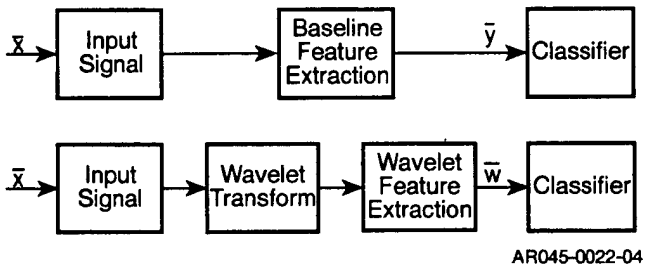


**Figure 18. Wavelet Transform as a Feature Extraction**

For this contract, feature sets were selected in a variety of ways. Several types of wavelets, several different sets of bases, and other feature selection techniques were investigated. The Haar wavelet, D02, and the Daubechies, D04, wavelet were extensively studied. The choice of the basis was based on different criteria. Some of these choices are listed in Table 4. The method described by Coifman and Wickerhauser [1,2] using the minimum entropy cost was examined. The Karhunen-Loeve criteria for selecting features was another technique tested. A method of reducing the feature set was created by quantifying the impact on classifier performance with and without a particular feature. Features with a large impact were considered important. This approach showed relationships between wavelet coefficients from various resolution levels. These different approaches to feature extraction are described in greater detail in Section 4.0 and in the performance results in Appendix A.

**Table 4. Feature Extraction and Classifier Options**

| Wavelet | Criterion | Classifier |
|---|---|---|
| D02 | Minimum entropy | Quadratic |
| D04 | Karhunen-Loeve | Quadratic Polynomial |
| D06 | Individual Feature | Profile Matching |
| • | • | Fusion |
| • | • | • |
| • | • | • |

Once the feature set was developed, the classifier itself was considered. Several different approaches to classification were tested. These included the quadratic classifier, quadratic polynomial classifier, profile matching, and combined classifiers using a fusion approach.

## 3.1 Quadratic Classifier

The quadratic classifier used is based on the Mahalonobis distance from each of the training data sets. For each of the classes involved in the decision, a set of training data samples from which an estimate of the class population mean and covariance is computed. These statistics are used since the population mean and covariance would determine the distribution if the population were indeed Gaussian. For each training class, a mean ($\overline{m}$) and a covariance ($\Sigma$) is computed. The testing stage of the process is based on computing the class which has the minimum distance from the test sample $\overline{x}$. This distance is given by $(\overline{x} - \overline{m}_i)^t \Sigma_i^{-1} (\overline{x} - \overline{m}_i) + \ln |\Sigma_i|$. The class which yields the minimum distance for the above is chosen as the assigned class.

## 3.2 Quadratic Polynomial Classifier

Another technique used a quadratic polynomial to build a decision surface. This was accomplished by computing powers and products of individual features and forming new feature vectors from these expanded terms. For each class, a coefficient vector $\overline{a}$ is formed. The individual training sample vectors $\overline{x}_{ij}$, $i^{th}$ class, and $j^{th}$ sample have been expanded to include the additional square and product terms. Let $X_i^t = \{\overline{x}_{i1}, ..., \overline{x}_{iM}\}$, M sample vectors from the $i^{th}$

class, and let $X^t = (X_1^t, ..., X_L^t)$ correspond to L classes. Then the coefficient vector is given by $\bar{a}_i = (X^tX)^{-1}\ \bar{m}_i$. The test vector and the coefficient vector are multiplied using the dot product $\bar{a}_i^t \cdot \bar{x}$. This value is compared to the threshold. If the value is greater than or equal to the threshold it corresponds to one class, and if less than the threshold to the other. This produces the quadratic polynomial surface in the feature space. For more than two classes, the decision logic is modified to allow for multiple surfaces.

### 3.3 Profile Matching Classifier

The profile matching (PM) approach is based on the nearest neighbor concept. A collection of vectors from each training set is stored and compared directly with the incoming sample. This comparison uses the distance $P_i$, with $P_i = \Sigma\ |x_i - s_{im}|$ where $x_i$ is the $i^{th}$ component of the test vector $\bar{x}$ and $s_{im}$ is the $i^{th}$ component of the $m^{th}$ stored training vector $\bar{s}_m$. The minimum distance is determined over all the stored samples and the decision is to choose the class of that sample which gave the minimum distance. This approach is computationally intensive if the space has high dimension and the number of stored samples is large.

### 3.4 Fusion Classifier

Performance for the individual classifiers can sometimes be improved if these techniques are combined into a fusion approach. The combination of the quadratic classifier and the profile matching classifier serves to illustrate this technique. The classifiers are constructed as described above, but additional information is needed. For both the quadratic classifier and the profile matching classifier, the distance which was second smallest is saved and the minimum distances are compared to the second smallest distances. Intuitively, the minimum distance that is further away from its second smallest distance provides the greatest decision confidence. This is the decision of the fusion classifier.

Since these classifiers have such different forms, it was determined that a multiplication factor was required for the profile matching distances to make the distances have comparable

values and achieve a valid fusion technique. For the fusion technique to be effective, the two approaches used must have comparable performances. Otherwise, the one classifier will dominate the other classifier in the fusion decision.

# 4.0 TECHNICAL RESULTS

Application of wavelet concepts to the radar ATR problem required incorporation of wavelet software into the ATR suite of algorithms. This adaptation was facilitated by the use of the software provided from FMA&H. The test focused on the modification of the feature set to incorporate wavelets and the classifier design. The goal was to build a feature set and classifier design with both improved performance and computational simplification, then to extend this approach to other parts of the ATR processing.

Initially, the extensive turntable database developed for Longbow was used. It includes many target types with ample azimuth and depression angle variation. The data was altered by the coherent addition of actual clutter from selected sites to better represent realistic environmental conditions. Later, the experimental database was expanded to include flight target data collected during actual system flights. This data is more representative of expected conditions, since it contains actual flight system data. The Longbow POP system was used for data collection.

The software provided by FMA&H contained both wavelet packet and multi-resolution analysis approaches for performing wavelet decomposition and reconstruction. These alternative methods were examined for advantages and disadvantages, both in the ease of use and their relative performance. An in-house wavelet software suite was built and modified to match up with the format of the data sets. This modification reduced input/output operations, which were adding significantly to the computational time for processing the data. The FMA&H software remains more efficient for analysis of a small number of ASCII signals, but for the large data files we were processing, the fixed approach proved more efficient.

## 4.1 Wavelet Classifier Results

Daubechies 2, 4, and 6 (D2, D4, and D6) wavelet coefficients were tested as features for a quadratic three-class target classifier algorithm. In general, the results were very similar among the three types of wavelet transform coefficients tested. Consequently, attention was focused on the D2 coefficients, since they can be calculated most efficiently.

Blind testing of the target-on-turntable data sets yielded average $P_{CC}$ values that were 6.7 percentage points higher than the Longbow baseline. The training set and the testing set consisted of radar looks at 360 degrees of aspect, at different elevation angles, with various levels of clutter added to the targets. These results were for a wavelet quadratic classifier that required 13.6 times more computations than the Longbow baseline classifier algorithm.

The major interest then became the testing of some of the flight data based on wavelet algorithms that were trained on turntable data and some of the other flight data. This is also blind testing because the training set and the testing set do not overlap. These results are generally indicative of what an operational system will experience.

The most recent wavelet classifier experiments used target-on-turntable data and some of the target flight data to train the classifier. The target data used to test the classifier was target flight data. The target flight test data set and the target flight training data set did not have any data in common; however, target aspect angles for flight test data were somewhat similar to target aspect angles for flight classifier training data. Also, target sites and adjacent clutter were similar for flight training data and flight test data. Consequently, some classifier performance enhancement was expected by adding the flight training data to the turntable data, for classifier training, due to a combination of similar clutter types and similar aspect angles between training data and testing data.

Tradeoffs and experiments were conducted to quantify some of the improvements in classifier performance through the use of flight training data in addition to turntable data. More importantly, the new wavelet-based classifiers outperformed the baseline Longbow POP classifier on flight test data. The Longbow POP classifier flight test database consisted of target data from four different Army test areas. Because each test area provided both near distance and far distance target data, a total of eight target test collections were available. There are four target types, which are denoted CL1, CL2, CL3, and CL4. The classifier will eventually merge CL3 and CL4 into one class; consequently, there are three final classes to contend with in the Longbow classifier associated with this data.

Classifier results are detailed in Appendix A and can be summarized in two ways. Both methods calculate the percent correct classification ($P_{CC}$) for each of the three target classes, using the eight target test collections. $P_{CC}$ values are given as deltas from a fixed, unreported $P_{CC}$ for reasons of classification. Method one (M1) calculates the (equally weighted) average of the three $P_{CC}$ values for each target test collection (except at the HL site, where only CL1 and CL2 target types are present). Then, these eight average $P_{CC}$ values are averaged to get a global average $P_{CC}$. Method two (M2) computes the sample size weighted average of the three $P_{CC}$ values for each target test collection. (This calculation yields the number of correct classifications/number of classifications ratio for each target test collection.) The eight sample weighted $P_{CC}$ averages are averaged to get a global average $P_{CC}$ (Avg. $P_{CC}$).

A case can be made for each of the two methods, but method one seems to work better. There are many more test samples from CL1 than from CL2, CL3, and CL4; so a poor, unbalanced classifier that favors CL1 yields better M2 scores than a good, more balanced classifier. This imbalance is illustrated by the poor M1 results in case 4 of Appendix A and the good M2 results in case 42 of Appendix A for an unsatisfactory classifier that changes all CL3 and CL4 calls to CL1 so that nothing is ever called final class 3. That is, this classifier should produce poor results by any appropriate scoring method.

Several conclusions follow from the analysis of the data in Appendix A:

1) Cases 1 and 39 contain M1 and M2 Longbow baseline classifier results.
2) Cases 2, 3, 40, and 41 appear to show that limiting turntable training data to the same target aspect angles as those of the flight training data, which are similar to the flight testing data, produces results which are not as good as the baseline in cases 1 and 39. These tests were designed to investigate a suspicion that including flight data in the training set led to better results because of target aspect angle similarities between the flight training data and testing data. The results are not conclusive, though, especially since some of the resulting classifier training sets suffered from small sample size

problems, which can cause the use of inappropriate inverse covariances in quadratic classifiers.

3) Cases 5 and 43 show that the baseline classifier biases, or gains, gave better results than the case in which zero biases were used. Comparison of case 6 with case 7 and case 44 with case 45 shows that the baseline weights also help W48, which is a D2 wavelet quadratic classifier using all wavelet coefficients except the highest frequency coefficients.

4) Comparison of case 7 with case 1 and case 45 with case 39 shows that the quadratic D2 wavelet classifier W48, which is 48-dimensional, works at least as well as the baseline classifier.

5) Cases 8 and 48 show that the 42-dimensional quadratic wavelet classifier W42, which consists of 24 D2 wavelet coefficients and 18 D2 wavelet packet coefficients, also works at least as well as the baseline classifier. In fact, W42 is at least as good as W48 and requires fewer quadratic classifier calculations.

6) Case 46 shows that a 26-dimensional wavelet classifier, which worked well in a target versus man-made object test, does not work well as the classifier. The reason may be that most of the man-made objects encountered were, in general, not as long as the target and the 26-dimensional wavelet classifier emphasized wavelet coefficients that correspond to central portions of the HRRP profile of the detected object.

7) Statistical analysis showed that the flight data included heavier clutter than the turntable data. Cases 11, 51, and 52 show that attempts to artificially adjust the turntable training data for heavier background clutter had no beneficial effect on classifier performance.

8) Cases 19, 20, 59, and 60 show that new versions of the original wavelet quadratic classifiers W48 and W42 (LPTRAIN will accompany the data in Appendix A for these new versions) can be designed that require far fewer computations than the original versions but still perform better than the baseline classifier. Implementation would allow computational reserves that can be used in the profile matching part of a sensor-fusion-

logic quadratic and profile-matching fusion classifier so that the fusion classifier requires no more computational capability than the baseline classifier. (In general, if very many training profiles are used in a profile matching classifier, the profile matching classifier requires many more computations than a quadratic classifier.) Some wavelet quadratic classifiers had a problem with a low $P_{CC}$ for class number three. These new versions made the problem worse.

9) Cases 23 and 63 show that the performance of an appropriate profile-matching classifier is better than the baseline results in cases 1 and 39.

10) Cases 28 and 68 show that a fusion classifier that combines a profile-matching classifier and the new W42 quadratic classifier produce average $P_{CC}$ values that are 3 percentage points better in the M1 sense and 5 percentage points better in the M2 sense than the baseline classifier. This fusion classifier is no more complex than the baseline classifier.

11) Cases 38 and 78 show the improved results versus cases 19 and 59 of a version of the new W42 quadratic classifier with branching logic based on the odd/even polarization ratio and a standard deviation statistic related to target length. The computational complexity of this version of the new W42 is similar to that of the case 19 and case 59 version of W42 (still much less than the baseline) and is therefore still compatible with fusion processing. That is, this branching version of W42 offers improved $P_{CC}$ performance without increasing the number of computations.

In conclusion, the two best wavelet classifiers produced on this project are wavelet fusion classifiers that are significantly better than the Longbow baseline classifier in terms of average $P_{CC}$, and both choices require no more computation than the Longbow baseline classifier. These are branching classifiers that fuse a profile-matching and a quadratic classifier.

Cases 30 and 70 show that a branching classifier that fuses a profile matching classifier and a W42 quadratic classifier produce average $P_{CC}$ values that are 4 percentage points better in the M1

sense and 6 percentage points better in the M2 sense than the baseline classifier. Details of this classifier are given in the comments at the top and the right of cases 30 and 70 in Appendix A.

Since merged class 3 may be the most important class, a modification was made to the previous fusion classifier. This new fusion classifier uses only the profile matching classifier in the branch where the odd/even ratio is high. The $P_{CC}$ values for this fusion classifier (cases 31 and 71) are 3 percentage points better than the baseline in both the M1 and the M2 sense, and the merged class 3 $P_{CC}$ values are at least as high as those of the baseline. Details of this classifier are in the comments at the top and the right of cases 31 and 71 in Appendix A.

One final issue that was addressed is the difference between turntable data and flight data. In the training of classifier algorithms, it has been the desire of ATR algorithmists to be able to use only turntable data for training and then test with flight data. This, of course, requires robust algorithms. To begin to address this issue for the classifier, it was decided to compare the means of the HRRP vectors for flight and turntable data. Figures 19 through 22 are plots of these data. Each plot is for a single target type and presents the even, cross, and odd polarization HRRP vectors. This data is from one sector of the 360-degree-possible azimuth aspect angle. The solid line is the turntable-only data, and the dashed line is the flight-only data. The plots appear reasonably similar. Plots from other sectors showed similar trends. There does not appear to be any reason to believe that flight and turntable HRRPs are drastically different.

## 4.2 HRRP Wavelet Registration Algorithms

HRRP target registration is the task of preparing for pattern recognition algorithms by electronically moving the profile to center it in the range bin. This is shown in Figure 23, where the solid line shows the original data with the target at the edge of the range bin and the dashed line shows the results of registration. Registration precedes the detection and discrimination algorithms. Consequently, performance of the registration algorithm has a great impact on the algorithms in

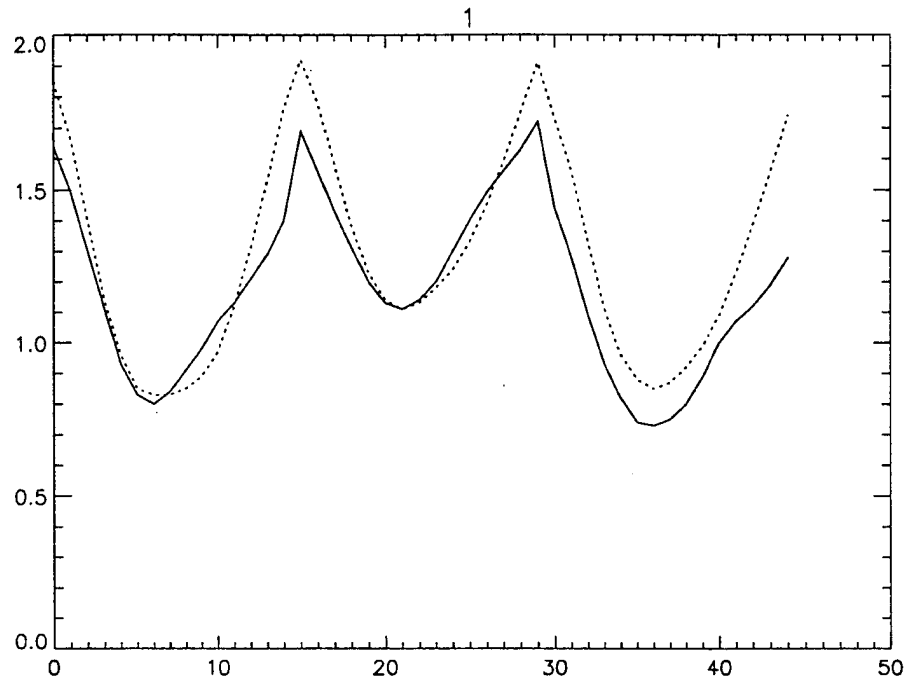


**Figure 19. Comparison of Mean Values of HRRP Polarization Vectors for Target Type 1**

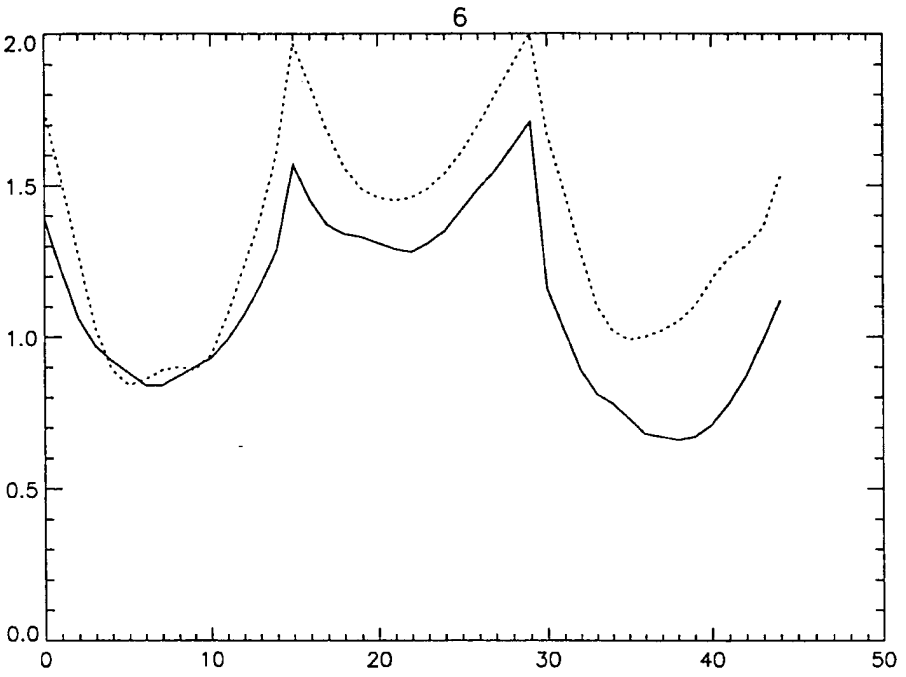


**Figure 20. Comparison of Mean Values of HRRP Polarization Vectors for Target Type 2**

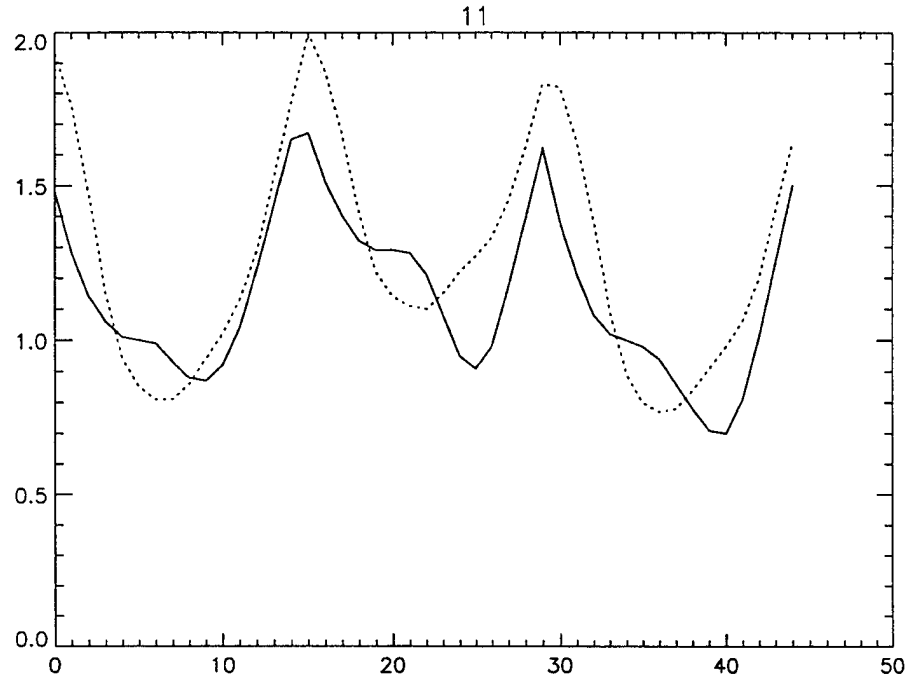


**Figure 21. Comparison of Mean Values of HRRP Polarization Vectors for Target Type 3**

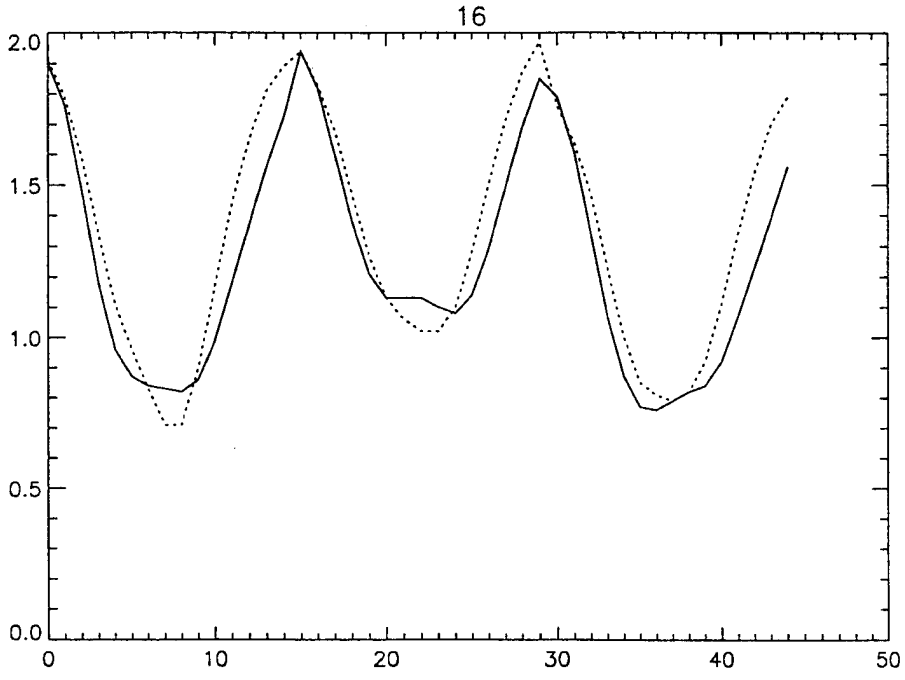


**Figure 22. Comparison of Mean Values of HRRP Polarization Vectors for Target Type 4**

each of these three parts of the FCR ATR. Registration is required for several reasons. First, the target may occupy only part of the HRRP from a given range bin. Second, the target-to-sensor range is often decreasing, so that there is a uniform probability that the target will be located anywhere within the range bin. Third, for most processing, the algorithms assume the target is centered in the range bin. Consequently, registration must estimate the center of the target, or the start and/or stop of the target, or some other locator of the target. The target may be split in the HRRP; if so, registration must correctly combine the split parts of the target. Both of these registration tasks are illustrated in Figure 23 for a target embedded in light clutter. That target, which was originally split and not centered in the HRRP, is combined correctly and centered in the HRRP by the registration algorithm.

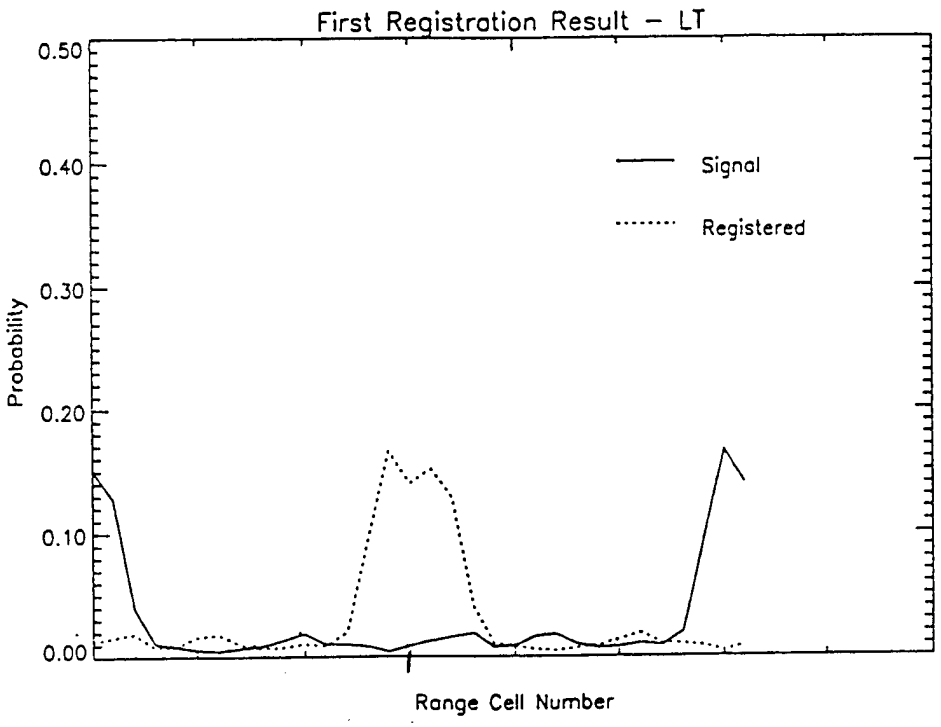


**Figure 23. Registration Example**

To create a "good" registration algorithm, one must first define what "good" means. The most appropriate definition is that a good registration algorithm improves target/clutter discrimination, target/MMO discrimination, and target classification performance. Unfortunately,

to compare registration algorithms, performance results must be compared for the three ATR tasks for the competing registration algorithms on the turntable and flight data. This task is an extremely time-consuming computer task and is not feasible unless faster registration comparison methods first narrow the candidate registration algorithms to a very few.

To illustrate why registration is important, an experiment was conducted in which the targets were always centered in the HRRP and no additional registration was needed. (This was possible because the turntable data was originally taken with the target on the center of the turntable and the turntable positioned so that the center of the turntable coincided with the center of the HRRP.) The Longbow baseline classifier was trained and tested on such data and the average $P_{cc}$ was 9.16 percentage points better than the same classifier with the Longbow baseline registration algorithm used, as usual. This experiment indicated that large ATR performance improvements are possible if registration can be significantly improved, especially if the registration accurately estimates the physical center of the target.

Two fast methods of evaluating registration algorithms were defined. One method was that if the same target was embedded in both light and heavy clutter, a good registration algorithm would provide the same target location for both cases. That is, the registration algorithm would not vary with background clutter level. One wavelet registration algorithm performed better than the Longbow baseline registration method in this sense. Figure 24 shows the results of registering an HRRP target embedded in both light (LT) and heavy (HV) clutter. This wavelet registration algorithm centers both versions of the same target in the same place. Table 5 summarizes the results of this investigation by comparing the wavelet registration with the standard registration as a function of light and heavy clutter as well as for two target types (T and W) and for two depression angles (low and high). In all cases, the wavelet registration was more robust.

However, when the baseline classifier and the wavelet baseline classifier were preceded with this wavelet registration method rather than the baseline registration method, average $P_{cc}$ dropped by 1 percentage point for both classifiers. It is not clear whether this is due to the current

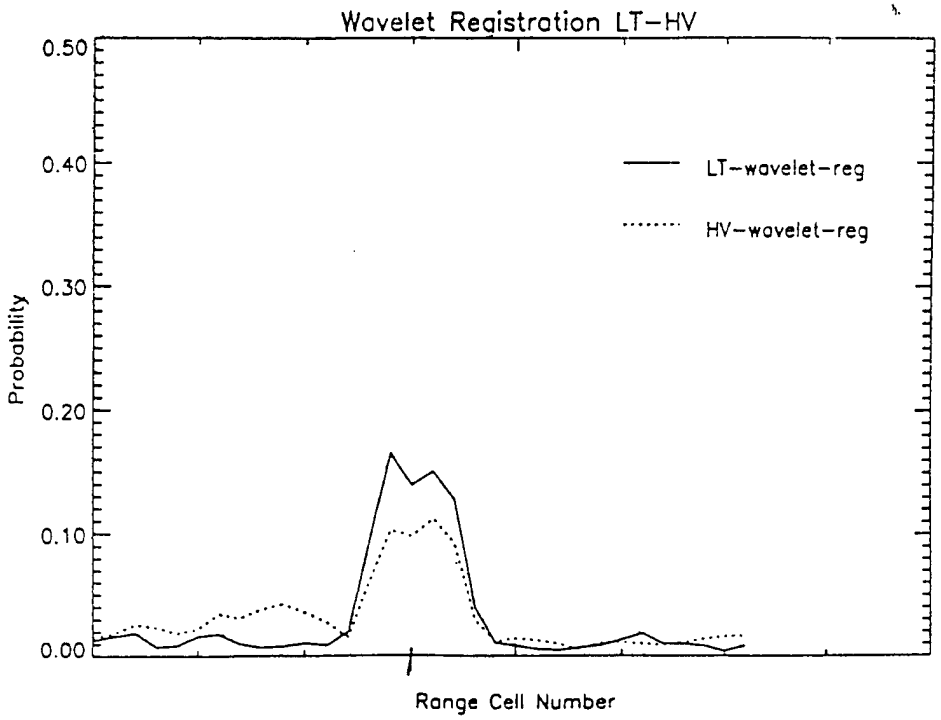


**Figure 24. Registration with Light and Heavy Clutter**

**Table 5. Registration Summary**

| | Average Heavy - Light | | |
|---|---|---|---|
| **Target Type** | **Reg** | **Wav** | **Imp (%)** |
| T-Low | 0.791 | 0.639 | 19.2 |
| T-High | 0.890 | 0.718 | 19.3 |
| W-Low | 0.374 | 0.287 | 23.3 |
| W-High | 0.879 | 0.736 | 16.3 |
| **Average** | **0.734** | **0.595** | **19.5** |

algorithms being adapted to account for the anomalies in registration or is an issue with the registration itself. It was concluded that this light/heavy clutter invariance measure was not a good enough fast method for evaluating registration algorithms.

The other fast method proposed to evaluate registration methods was to measure how well the registration method finds the known center of the turntable. In the Longbow turntable data files, the target HRRP has been randomly shifted so that the center of the HRRP is generally not the center of the turntable and different levels of clutter have been added to the target. However, it

is possible to retrieve the original center of the turntable position in this shifted HRRP, for registration testing purposes. This evaluation method showed that a perfect registration method that always picks the center of the turntable yields an average 9.16 percentage points improvement in the classifier $P_{CC}$. Also, a registration algorithm that was somewhat better than the Longbow baseline registration algorithm in this sense did show some improvement in classifier average $P_{CC}$. This evaluation method requires about 1.5 minutes of computer time to run, while the classifier requires several hours to run. It appears that this evaluation method is a suitable fast registration evaluation tool.

### 4.3 Target - Clutter ATR Results

Examination of the Longbow target versus clutter discrimination process was initiated. This process is a complex sequence of different types of discrimination algorithms where, typically, the output of one algorithm becomes the input to the next. The types of data required for the different algorithms vary, and the types of computer files vary also. An additional complication is that the data files are very large, so considerable disk space must be allocated for this discrimination study. The appropriate (archived) data files and existing software for processing these files have been identified. Wavelet software will need to be integrated into this software, and new algorithms will need to be designed and tested to see whether wavelet techniques can improve target/clutter discrimination.

### 4.4 Wavelet Target - MMO ATR Results

D2, D4, and D6 wavelet coefficients have been tested as features for a quadratic MMO target versus man-made object discrimination algorithm. In general, the results were very similar among the three types of wavelet coefficients tested. Consequently, attention was focused on the D2 coefficients, since they can be calculated most efficiently.

Resubstitution testing of the APG, HL, WSMR, and YPG flight data sets of targets and man-made objects yielded average $P_{CC}$ values that were just over 7 percentage points higher than

the Longbow baseline. Resubstitution results are considered to be optimistic, since the algorithm training set is the same as the algorithm testing set. Of more interest was the testing of some of the flight data based on wavelet algorithms that were trained on turntable data and some of the other flight data. This blind testing uses a training set and testing set that do not overlap. These results are generally indicative of what an operational system will experience.

The data that the MMO algorithms were tested against was flight MMO and target data from the four test sites discussed in Section 4.1: APG, HL, WSMR, and YPG. Results are given in terms of $P_{CC}$ change (versus the Longbow baseline MMO algorithm) for the two classes (target and MMO) for each of the four sites. The results given in Table 6 are $P_{CC}$ values for the two-class problem and are presented for the four sites. The results are all relative to the Longbow baseline target MMO algorithm. Some description of the wavelet algorithms that were tested is included. The wavelet baseline in Table 6 uses all D2 coefficients except the coefficients corresponding to the wavelet functions with the highest wavelet frequency (shortest length).

These results show that a new wavelet target-MMO algorithm can increase average $P_{CC}$ versus the Longbow baseline by 7.53 percentage points and simultaneously reduce the number of computations required to about one-third of the number required by the Longbow baseline MMO algorithm.

## 4.5 SAR Wavelet Algorithms

SAR images were provided by Lincoln Labs. The data provided was:

Mission 85 pass 5, frames 27-30

Mission 90 pass 5, frames 1-127

Mission 78 pass 1, frames 5-40

Mission 78 pass 2, frames 16-42

Mission 78 pass 3, frames 1-38

Mission 78 pass 4, frames 6-27

**Table 6. Target - MMO $P_{cc}$ Results and Algorithm Complexity**

| Target | MMO | Rel. Avg. $P_{cc}$ | Complexity | Comments |
|---|---|---|---|---|
| 0.00 | 0.00 | | | Longbow Baseline |
| 0.00 | 0.00 | | | |
| 0.00 | 0.00 | | | |
| 0.00 | 0.00 | 0.00 | 1.000 | |
| 5.03 | 0.79 | | | Wavelet Baseline |
| 14.01 | -2.61 | | | |
| 5.12 | 3.42 | | | |
| 4.89 | 4.24 | 4.36 | 1.136 | |
| 12.44 | -1.20 | | | Several features deleted from the Wavelet Baseline |
| 22.79 | -6.29 | | | |
| 7.26 | 1.42 | | | |
| 6.44 | 2.12 | 5.62 | 0.449 | |
| 15.37 | -3.65 | | | More features deleted from the Wavelet Baseline |
| 26.73 | -9.58 | | | |
| 6.64 | 0.26 | | | |
| 6.49 | 2.99 | 5.66 | 0.290 | |
| 22.77 | -6.61 | | | New transformation applied to the previous algorithm |
| 31.28 | -12.77 | | | |
| 5.44 | -1.32 | | | |
| 6.80 | 8.74 | 6.79 | 0.290 | |
| 22.80 | -6.84 | | | A few features deleted from the previous algorithm |
| 31.61 | -12.48 | | | |
| 5.85 | -1.37 | | | |
| 7.56 | 9.11 | 7.03 | 0.244 | |
| 23.25 | -7.29 | | | A few wavelet packet features added to the previous algorithm |
| 32.12 | -12.39 | | | |
| 5.90 | -0.90 | | | |
| 7.66 | 11.86 | 7.53 | 0.339 | |

Mission 78 pass 6, frames 6-26

Mission 78 pass 7, frames 12-41

Mission 78 pass 8, frames 7-32

Mission 78 pass 9, frames 5-41

Mission 85 pass 1, frames 1-38

Mission 85 pass 2, frames 5-37

Mission 85 pass 3, frames 7-42

Mission 85 pass 4, frames 1-32

Mission 85 pass 6, frames 1-37

Mission 85 pass 7, frames 1-41

Mission 85 pass 8, frames 1-31

Mission 85 pass 9, frames 1-31.

Each frame consists of four polarizations of I and Q data for images of 512 by 2058 pixels. Data collection was conducted at Stockbridge, NY. There are scenes containing both rural clutter and arrays of target objects. The targets represented are:

2 M-55 howitzers

2 M-60 tanks

3 M-48 tanks

1 M-113 armored personnel carrier

2 M-84 armored personnel carriers

1 M-59 armored personnel carrier.

Software was developed to read the raw data files provided and to create SAR images. Problems were overcome concerning construction of the edges of the SAR images and also concerning the splicing together of parts or subimages of one large SAR image. The data has been now been processed both as single polarization magnitude (pixel) data and also as complex I, Q data from multiple polarizations. The images that were processed appeared to be very clean. Objects that were known to be in the images were easily identified.

A whitening filter suggested by Dr. Les Novak from Lincoln Labs was coded and applied to one SAR image. The results of this filter appeared to be about a 30 percent improvement in the visual clarity of the image. Wavelet noise removal and image compression techniques were applied to one of these SAR images. The results were reasonably good, as was expected.

Two-dimensional wavelet code was written with the goals of easing filtering and compression, followed by inverse wavelet transformation to reconstruct the images. An algorithm was defined that used filtered coefficients from two-dimensional wavelet transforms to detect and register (in a two-dimensional SAR image as opposed to the previous one-dimensional HRRP) a target in a SAR image. The algorithm used the wavelet coefficients and did not require an inverse

wavelet transformation. This algorithm exploits the expected correlations of multiple target pixels in the SAR image. The algorithm was very effective at locating targets in the SAR database. Also, an artificial target was imbedded in heavy noise where the peak noise was higher than the peak signal. The wavelet coefficient detection and registration algorithm had no trouble locating this target in spite of the very heavy noise. The algorithm uses the known surface locations corresponding to the coefficients selected by the algorithm (and does not use the scaling function's coefficient) to compute the target's location by probability methods.

At this point, this effort was terminated by direction from the ARPA Program Manager in favor of concentrating on range-only radar processing.

### 4.6 Software Developed

Classifier software was created for target-MMO algorithm evaluation. Software was written to read Lincoln Labs SAR data and to construct the images. SAR processing software was created to fix edge problems in earlier SAR image creation programs. Also, new software was created to correctly combine parts of the large SAR images into the complete images. Two-dimensional wavelet transform programs were written to allow easy filtering of coefficients and fast sorting for coefficient selection or image compression. Inverse transform code was also written.

All of the two-dimensional code is as fast as possible, requires no external library links, and therefore could be transferred to any computer (such as PC or Sun workstation) that has a FORTRAN compiler. Code was written to test wavelet HRRP registration algorithms, perform wavelet detection and registration on SAR images, whiten SAR images, return Longbow target data to the center-of-turntable (perfect registration) position, and to quantify the benefits of perfect registration.

## 4.7 Fast Mathematical Algorithms and Hardware Corporation

Fast Mathematical Algorithms and Hardware Corporation has collaborated over the last few years with the Martin Marietta radar group directed by Charles Stirman in Orlando, Florida, for processing radar returns for automatic target recognition tasks using wavelet-based technology.

FMA&H's role in this work was principally to provide Martin Marietta with the latest developments in signal processing tools, as well as to assist in adapting these tools to the needs of Martin Marietta. In particular, methods developed at Yale, New York University (NYU), and other research centers were organized into a comprehensive toolkit. FMA&H performed these tasks from 1992-1995:

1) Converted and delivered properly debugged and documented transportable wavelet and wavelet packet signal processing development environment to VAX/VMS and Sun operating system at Martin Marietta's Orlando facility. This code incorporates the Wavel code of Mallat at NYU as well as the wavelet-packet code developed at Yale and FMA&H. This development environment is being continuously upgraded and expanded to include higher dimensional signal processing.
2) Organized and presented two workshops to instruct Martin Marietta personnel (as well as other government lab personnel) in usage of the algorithms and software.
3) Produced and delivered instructional material to train users, analysts, and programmers in the use of the wavelet or wavelet-packet-based signal processing development and simulation software.
4) Provided continuous technical support, consulting, and interactive algorithm development for various ATR tasks as required by Martin Marietta. These tasks included parameter extraction toolkits, denoising algorithms and software, and an initial exploration for automating the process of parameter extraction.

## APPENDIX A. WAVELET CLASSIFIER COMPARISON TABLE FOR 78 CASES

The following data contains results from 78 classifier experiments. Many other classifier experiments were run, but the results were not significant enough to report. Cases 1 through 38 contain M1 (equally weighted average) scoring results, and cases 39 through 78 contain M2 (sample size weighted average) scoring results. Some description of the experiments is given at the top and at the right side of each experiment's subsection in the data table. The eight "Average $P_{CC}$" numbers given in the tables are for near distance, followed by far distance testing data from APG, HL, WSMR, and YPG respectively. This notation is used throughout:

| | |
|---|---|
| QD | quadratic classifier |
| PM | profile matching |
| BD | Mahalanobis distance + ln determinant (QD discriminant) |
| BB | similar to BD except for PM classifier |
| O/E | total odd power divided by total even power |
| STD | standard deviation (large implies long target) |
| PM_DELTA | measure of PM classifier's confidence |
| Q_DELTA | measure of QD classifier's confidence |
| TT | target-on-turntable radar data |
| BIAS | number added to QD and PM calculations to shift $P_{CC}$ values |
| LPTRAIN | file name that indicates QD with few calculations |

Four original classes: CL1, CL2, CL3, CL4. CL3 and CL4 are eventually merged together

Results are relative to the baseline $P_{CC}$ from the Longbow algorithms, for comparison

+ indicates an improvement in relative performance in percent

- indicates a loss in relative performance in percent

Cases 1–38 weight 3-class $P_{CC}$ values equally

Cases 39–78 weight $P_{CC}$ values based on test sample sizes

For each of the cases, the file header identifies the individual data sources

**For each case, we present the average $P_{CC}$ for the near range and the far range at each test site in alphabetical order followed by the overall average:**

| LEGEND FOR EACH CASE |
|---|
| Aberdeen Proving Grounds – Near |
| Aberdeen Proving Grounds – Far |
| Ft. Hunter-Liggett – Near |
| Ft. Hunter-Liggett – Far |
| White Sands Missile Range – Near |
| White Sands Missile Range – Far |
| Yuma Proving Grounds – Near |
| Yuma Proving Grounds – Far |
| AVG. = Overall average for case |

**METHOD 1 SCORING RESULTS**

1. BASELINE CLASSIFIER GAINS (BL)

Average $P_{CC}$ = +11

Average $P_{CC}$ = -11

Average $P_{CC}$ = +6

Average $P_{CC}$ = +6

Average $P_{CC}$ = +13

Average $P_{CC}$ = +6

Average $P_{CC}$ = +6

Average $P_{CC}$ = -2

AVG. = +4 (+4.4)

Average of merged class 3 $P_{CC}$ values = +0.0

2. [LPEELE.FLIGHT.FILES]TRAIN_BL_ANG_TT.PRM

| | | |
|---|---|---|
| Average $P_{CC}$ = | +3 | |
| Average $P_{CC}$ = | -19 | Train on turntable data at |
| Average $P_{CC}$ = | +8 | same aspects as flight |
| Average $P_{CC}$ = | +5 | training data - small sample |
| Average Pcc = | +2 | sizes for some sectors |
| Average $P_{CC}$ = | -4 | |
| Average $P_{CC}$ = | -3 | |
| Average $P_{CC}$ = | -9 | |
| AVG. = | -2 | |

3. [LPEELE.FLIGHT.FILES]TRAIN_BL_ANG.PRM

| | | |
|---|---|---|
| Average $P_{CC}$ = | +7 | |
| Average $P_{CC}$ = | -9 | Turntable data at flight |
| Average $P_{CC}$ = | +7 | training aspects plus |
| Average $P_{CC}$ = | +3 | flight training data |
| Average $P_{CC}$ = | +9 | |
| Average $P_{CC}$ = | +2 | |
| Average $P_{CC}$ = | +4 | |
| Average $P_{CC}$ = | -6 | |
| AVG. = | +2 | |

4. BASELINE CLASSIFIER GAINS: THEN MERGED CLASS 3 CALLS FORCED INTO CLASS 1

| | | |
|---|---|---|
| Average $P_{CC}$ = | +0 | |
| Average $P_{CC}$ = | -18 | |
| Average $P_{CC}$ = | -5 | This poor average result shows the |
| Average $P_{CC}$ = | -9 | results of the three $P_{CC}$ values being equally |
| Average $P_{CC}$ = | +2 | weighted rather than weighted by |
| Average $P_{CC}$ = | -2 | sample size, as in 42.) |
| Average $P_{CC}$ = | -6 | |
| Average $P_{CC}$ = | -9 | |
| AVG. = | -6 | |

5. CLASSIFIER GAINS: 0.00 0.00 0.00 0.00

Average $P_{CC}$ = +7

Average $P_{CC}$ = -10

Average $P_{CC}$ = -1

Average $P_{CC}$ = +0

Average $P_{CC}$ = +11

Average $P_{CC}$ = +4

Average $P_{CC}$ = +6

Average $P_{CC}$ = -4

AVG. = +2

6. [LPEELE.FLIGHT.FILES]TRAIN_W48.PRM NO WEIGHTS (ALL ZERO)

Average $P_{CC}$ = +0

Average $P_{CC}$ = -11

Average $P_{CC}$ = +4

Average $P_{CC}$ = +2

Average $P_{CC}$ = +12

Average $P_{CC}$ = +8

Average $P_{CC}$ = +2

Average $P_{CC}$ = -1

AVG. = +2

7. [LPEELE.FLIGHT.FILES]TRAIN_W48.PRM WEIGHTS = BL WEIGHTS

(Average $P_{CC}$ = + 6)

Average $P_{CC}$ = -12

Average $P_{CC}$ = +8

Average $P_{CC}$ = +9

Average $P_{CC}$ = +12

Average $P_{CC}$ = +7

Average $P_{CC}$ = +3

Average $P_{CC}$ = -2

AVG. = +4

8. [LPEELE.FLIGHT.FILES]TRAIN_W42.PRM

Average $P_{cc}$ = +6

Average $P_{cc}$ = -10

Average $P_{cc}$ = +7

Average $P_{cc}$ = +9

Average $P_{cc}$ = +14

Average $P_{cc}$ = +8

Average $P_{cc}$ = +5

Average $P_{cc}$ = +0

AVG. = +5

9. [LPEELE.FLIGHT.FILES]TRAIN_W42_F_ONLY.PRM

Average $P_{cc}$ = +1

Average $P_{cc}$ = -8

Average $P_{cc}$ = +15

Average $P_{cc}$ = +6

Average $P_{cc}$ = +5

Average $P_{cc}$ = +4

Average $P_{cc}$ = +1

Average $P_{cc}$ = -12

AVG. = +2

10. [LPEELE.FLIGHT.FILES]TRAIN_W42_TT_ONLY.PRM

Average $P_{cc}$ = -4

Average $P_{cc}$ = -16

Average $P_{cc}$ = +0

Average $P_{cc}$ = +1

Average $P_{cc}$ = +14

Average $P_{cc}$ = +5

Average $P_{cc}$ = +2

Average $P_{cc}$ = -4

AVG. = +0

11. [LPEELE.FLIGHT.FILES]TRAIN_BL_SP.PRM

| | | |
|---|---|---|
| Average $P_{cc}$ = | +7 | |
| Average $P_{cc}$ = | -7 | |
| Average $P_{cc}$ = | +10 | Dependent clutter |
| Average $P_{cc}$ = | +9 | added to turntable |
| Average $P_{cc}$ = | +9 | training data |
| Average $P_{cc}$ = | +2 | |
| Average $P_{cc}$ = | +5 | |
| Average $P_{cc}$ = | -2 | |
| AVG. = | +4 | |

12. [LPEELE.FLIGHT.FILES]TRAIN_BL_SP_TT.PRM

| | | |
|---|---|---|
| Average $P_{cc}$ = | +0 | |
| Average $P_{cc}$ = | -15 | |
| Average $P_{cc}$ = | +4 | Same as case 11 above |
| Average $P_{cc}$ = | -1 | except train on |
| Average $P_{cc}$ = | +11 | turntable data only |
| Average $P_{cc}$ = | +1 | |
| Average $P_{cc}$ = | +2 | |
| Average $P_{cc}$ = | -6 | |
| AVG. = | +0 | |

13. [LPEELE.FLIGHT.FILES]LPTRAIN_BL_ANG.PRM

| | | |
|---|---|---|
| Average $P_{cc}$ = | +7 | |
| Average $P_{cc}$ = | -10 | One sector only, |
| Average $P_{cc}$ = | +14 | train on turntable data |
| Average $P_{cc}$ = | +9 | at same angles as |
| Average $P_{cc}$ = | +8 | flight training data |
| Average $P_{cc}$ = | +2 | |
| Average $P_{cc}$ = | +7 | |
| Average $P_{cc}$ = | +3 | |
| AVG. = | +5 | |

14. [LPEELE.FLIGHT.FILES]LPTRAIN_BL_ANG_TT.PRM

| | | |
|---|---|---|
| Average $P_{CC}$ = | +2 | |
| Average $P_{CC}$ = | -15 | |
| Average $P_{CC}$ = | +11 | Same as case 13 above except |
| Average $P_{CC}$ = | +10 | train on only turntable data |
| Average $P_{CC}$ = | +4 | |
| Average $P_{CC}$ = | +0 | |
| Average $P_{CC}$ = | +4 | |
| Average $P_{CC}$ = | -4 | |
| AVG. = | +2 | |

15. [LPEELE.FLIGHT.FILES]LPTRAIN_BL_ANG_TT.PRM

(Average $P_{CC}$ = + 2)

| | | |
|---|---|---|
| Average $P_{CC}$ = | -15 | |
| Average $P_{CC}$ = | +11 | |
| Average $P_{CC}$ = | +10 | Train on turntable data at |
| Average $P_{CC}$ = | +4 | flight training angles - |
| Average $P_{CC}$ = | +0 | use one sector only |
| Average $P_{CC}$ = | +4 | |
| Average $P_{CC}$ = | -4 | |
| AVG. = | +2 | |

16. [LPEELE.FLIGHT.FILES]LPTRAIN_BL.PRM

| | | |
|---|---|---|
| Average $P_{CC}$ = | +4 | |
| Average $P_{CC}$ = | -12 | Like baseline classifier except |
| Average $P_{CC}$ = | +14 | use only one sector |
| Average $P_{CC}$ = | +14 | |
| Average $P_{CC}$ = | +9 | |
| Average $P_{CC}$ = | +4 | |
| Average $P_{CC}$ = | +6 | |
| Average $P_{CC}$ = | +2 | |
| AVG. = | +5 | |

17. [LPEELE.FLIGHT.FILES]LPTRAIN_BL_TT.PRM

| | | |
|---|---|---|
| Average $P_{cc}$ = | +1 | |
| Average $P_{cc}$ = | -15 | Use one sector only, |
| Average $P_{cc}$ = | +10 | train on all turntable only |
| Average $P_{cc}$ = | +11 | |
| Average $P_{cc}$ = | +9 | |
| Average $P_{cc}$ = | +2 | |
| Average $P_{cc}$ = | +5 | |
| Average $P_{cc}$ = | -2 | |
| AVG. = | +3 | |

18. [LPEELE.FLIGHT.FILES]TRAIN_BL_TT.PRM

| | | |
|---|---|---|
| Average $P_{cc}$ = | +3 | |
| Average $P_{cc}$ = | -18 | |
| Average $P_{cc}$ = | +4 | Baseline except |
| Average $P_{cc}$ = | +3 | train on all turntable only |
| Average $P_{cc}$ = | +12 | |
| Average $P_{cc}$ = | +3 | |
| Average $P_{cc}$ = | +5 | |
| Average $P_{cc}$ = | -3 | |
| AVG. = | +1 | |

19. [LPEELE.FLIGHT.FILES]LPTRAIN_W42.PRM

| | | |
|---|---|---|
| Average $P_{cc}$ = | +1 | |
| Average $P_{cc}$ = | -10 | One sector only |
| Average $P_{cc}$ = | +14 | |
| Average $P_{cc}$ = | +13 | |
| Average $P_{cc}$ = | +13 | |
| Average $P_{cc}$ = | +5 | |
| Average $P_{cc}$ = | +3 | |
| Average $P_{cc}$ = | +1 | |
| AVG. = | +5 | |

20. [LPEELE.FLIGHT.FILES]LPTRAIN_W48.PRM

| | | |
|---|---|---|
| Average $P_{cc}$ = | +4 | |
| Average $P_{cc}$ = | -15 | One sector only |
| Average $P_{cc}$ = | +15 | |
| Average $P_{cc}$ = | +14 | |
| Average $P_{cc}$ = | +10 | |
| Average $P_{cc}$ = | +4 | |
| Average $P_{cc}$ = | +4 | |
| Average $P_{cc}$ = | +2 | |
| AVG. = | +5 | |

21. [LPEELE.FLIGHT.FILES]LPTRAIN_W42_REG.PRM

(Average Pcc = + 2)

| | | |
|---|---|---|
| Average $P_{cc}$ = | -10 | |
| Average $P_{cc}$ = | +13 | Second registration used, |
| Average $P_{cc}$ = | +10 | only one sector |
| Average $P_{cc}$ = | +13 | |
| Average $P_{cc}$ = | +5 | |
| Average $P_{cc}$ = | +3 | |
| Average $P_{cc}$ = | +0 | |
| AVG. = | +5 | |

22. [LPEELE.FLIGHT.FILES]PROFILE.PRM

| | | |
|---|---|---|
| Average $P_{cc}$ = | +8 | |
| Average $P_{cc}$ = | -10 | |
| Average $P_{cc}$ = | +1 | Profile matching baseline features except |
| Average $P_{cc}$ = | +5 | took 4th root, then normed by the |
| Average $P_{cc}$ = | +6 | square root of sum squares |
| Average $P_{cc}$ = | +0 | |
| Average $P_{cc}$ = | +5 | |
| Average $P_{cc}$ = | -3 | |
| AVG. = | +2 | |

23. [LPEELE.FLIGHT.FILES]PROFILE.PRM

CLASS 1 HAS A +0.001 BIAS

| | | |
|---|---|---|
| Average $P_{cc}$ = | +9 | |
| Average $P_{cc}$ = | -15 | |
| Average $P_{cc}$ = | +14 | |
| Average $P_{cc}$ = | +16 | Same as case 22 except class 1 |
| Average $P_{cc}$ = | +5 | has a bias of +0.001 |
| Average $P_{cc}$ = | +2 | |
| Average $P_{cc}$ = | +7 | |
| Average $P_{cc}$ = | +2 | |
| AVG. = | +5 | |

24. [LPEELE.FLIGHT.FILES]PROFILE.PRM

CLASS 1 HAS +0.0007 BIAS

| | | |
|---|---|---|
| Average $P_{cc}$ = | +12 | |
| Average $P_{cc}$ = | -14 | |
| Average $P_{cc}$ = | +11 | |
| Average $P_{cc}$ = | +15 | Same as case 22 except class 1 |
| Average $P_{cc}$ = | +8 | has a bias of 0.0007 |
| Average $P_{cc}$ = | +1 | |
| Average $P_{cc}$ = | +8 | |
| Average $P_{cc}$ = | +1 | |
| AVG. = | +5 | |

25. [LPEELE.FLIGHT.FILES]PROFILE_TT.PRM

CLASS 1 BIAS IS +0.001, TRAIN ON TURNTABLE ONLY

| | | |
|---|---|---|
| Average $P_{cc}$ = | +9 | |
| Average $P_{cc}$ = | -17 | |
| Average $P_{cc}$ = | +11 | Same as case 23 |
| Average $P_{cc}$ = | +8 | except trained on |
| Average $P_{cc}$ = | +6 | turntable only |
| Average $P_{cc}$ = | +1 | |
| Average $P_{cc}$ = | +6 | |
| Average $P_{cc}$ = | -2 | |
| AVG. = | +3 | |

26. [LPEELE.FLIGHT.FILES]LPTRAIN_W42.PRM - USUAL BIAS WEIGHTS ALSO USED PROFILE.PRM, FUSE CLASSIFIER - PM CLASS 1 HAS +0.001 BIAS

| | | |
|---|---|---|
| Average $P_{CC}$ = | +9 | Fuse classifier - fuse criterion |
| Average $P_{CC}$ = | -11 | is to use quadratic with usual |
| Average $P_{CC}$ = | +17 | weights unless (BDNEXT-BDMIN) < 2 ; |
| Average $P_{CC}$ = | +18 | then use profile matching. |
| Average $P_{CC}$ = | +11 | Currently there is no logic in the |
| Average $P_{CC}$ = | +3 | branching test for dealing with 2 |
| Average $P_{CC}$ = | +6 | target types being in the same class |
| Average $P_{CC}$ = | +3 | |
| AVG. = | +7 | |

27. [LPEELE.FLIGHT.FILES]LPTRAIN_W42.PRM

ALSO USED PROFILE.PRM, FUSE CLASSIFIER

| | | |
|---|---|---|
| Average $P_{CC}$ = | +10 | |
| Average $P_{CC}$ = | -12 | Same as case 26 except |
| Average $P_{CC}$ = | +17 | < 2 becomes < 2.8 |
| Average $P_{CC}$ = | +18 | |
| Average $P_{CC}$ = | +10 | This will use quad approximately 1/2 time |
| Average $P_{CC}$ = | +2 | |
| Average $P_{CC}$ = | +9 | |
| Average $P_{CC}$ = | +4 | |
| AVG. = | +7 | |

28. [LPEELE.FLIGHT.FILES]LPTRAIN_W42.PRM - USUAL BIAS WEIGHTS, ALSO USED PROFILE.PRM, FUSE CLASSIFIER - PM CLASS 1 HAS +.001 BIAS

| | | |
|---|---|---|
| Average $P_{CC}$ = | +8 | |
| Average $P_{CC}$ = | -11 | Uses PM (not QD) if |
| Average $P_{CC}$ = | +17 | 2500*PM_DELTA is > |
| Average $P_{CC}$ = | +18 | Q_DELTA; 2500 is |
| Average $P_{CC}$ = | +11 | approximately the ratio of |
| Average $P_{CC}$ = | +3 | the medians. |
| Average $P_{CC}$ = | +8 | |
| Average $P_{CC}$ = | +4 | |
| AVG. = | +7 | |

29. [LPEELE.FLIGHT.FILES]LPTRAIN_W42.PRM - USUAL BIAS WEIGHTS, ALSO USES PROFILE.PRM, FUSE CLASSIFIER - PM CLASS 1 HAS +.001 BIAS

Average $P_{CC}$ = +8

Average $P_{CC}$ = -11 Selects class based on

Average $P_{CC}$ = +18 minimum across classes of

Average $P_{CC}$ = +19 (QUAD BD + [(1-PM#)*2500])

Average $P_{CC}$ = +12 where the quad BD and the

Average $P_{CC}$ = +4 PM# are from the same class

Average $P_{CC}$ = +7

Average $P_{CC}$ = +3

AVG. = +8 (+7.5)

30. [LPEELE.FLIGHT.FILES]LPTRAIN42_ANGSECT.PRM FUSED WITH PROFILE MATCHING WITH CL1+0.001

Fusion is by minimum of (QD + 2500(1-PM))

Baseline classifier gains

Sectors are: Sect1 if O/E > 2.

Sect2 if not1 and std < 2.95

Sect3 if not1 and std > 2.95

Extra biases are Sect1&2 CL3-1; Sect3 CL1-1, CL2-2

This classifier has the best M1 and M2 results.

Average $P_{CC}$ = +8

Average $P_{CC}$ = -9

Average $P_{CC}$ = +18

Average $P_{CC}$ = +20

Average $P_{CC}$ = +13

Average $P_{CC}$ = +4

Average $P_{CC}$ = +9

Average $P_{CC}$ = +4

AVG = +8 (+8.4)

Average of merged class 3 $P_{CC}$ values = - 12.2

31. [LPEELE.FLIGHT.FILES]LPTRAIN42_ANGSECT.PRM & PROFILE.PRM

Sectors are: Sect1 if O/E > 2. [PM (not fusion) used in sect], Sect2 if not1 and std < 2.95, Sect3 if not1 and std > 2.95; baseline classifier gains; extra quadratic biases are Sect2 CL3&4-1, CL2+2; Sect3 CL1-1, CL2-2; profile matching biases are CL1+.001, CL3+.0005; BD(i) = Q(i) and BB(i) = (1 -PM(i))*2500 for i =1, ..., 4

Then BD(3) = min(BD(3),BD(4)) & BB(3) = min(BB(3),BB(4)) [which forces CL4–>CL3 to combine the two]; fuse by minimum of 3 classes BD(1)+BB(1)-.5 , BD(2)+BB(2) , BD(3)+BB(3)-1

This classifier has good class 3 $P_{CC}$ and good M1 & M2 results.

Average $P_{CC}$ = +7

Average $P_{CC}$ = -7

Average $P_{CC}$ = +12

Average $P_{CC}$ = +14

Average $P_{CC}$ = +14

Average $P_{CC}$ = +3

Average $P_{CC}$ = +9

Average $P_{CC}$ = +5

AVG. = +7

Average of merged class 3 $P_{CC}$ values = + 0.3

32. DIAGONAL COVARIANCE Q - 90 SECTORS - [POOR RESULTS]

33. DIAGONAL COVARIANCE Q - 90 SECTORS - **.25 NORMALIZATION [LPEELE.FLIGHT.FILES]DIAGTRAIN.PRM

Class 1 has a - 5 bias

Average $P_{CC}$ = +11

Average $P_{CC}$ = -12 Classifier assumes independence

Average $P_{CC}$ = +5 which is clearly not true

Average $P_{CC}$ = +14

Average $P_{CC}$ = +10 Baseline lines / SSQ-all

Average $P_{CC}$ = +3 then **0.25

Average $P_{CC}$ = +3

Average $P_{CC}$ = -3

AVG. = +4

34. [LPEELE.FLIGHT.FILES]LPTRAIN_ANGSECT.PRM

3 sectors based on even st.dev. statistic - even f(i)/|f| classifier gains altered slightly for 3 sector st.dev. distributions, baseline classifier gains plus alterations

| | | |
|---|---|---|
| Average $P_{CC}$ = | +4 | |
| Average $P_{CC}$ = | -10 | 3 sectors A,B,C are |
| Average $P_{CC}$ = | +13 | A if std < 2.65 |
| Average $P_{CC}$ = | +14 | B if 2.65 < std < 2.95 |
| Average $P_{CC}$ = | +10 | C if 2.95 > std |
| Average $P_{CC}$ = | +2 | A bias is CL3-1 |
| Average $P_{CC}$ = | +11 | C biases are CL1-1, CL2-2 |
| Average $P_{CC}$ = | +3 | |
| AVG. = | +6 | |

35. [LPEELE.FLIGHT.FILES]LPTRAIN_ANGSECT.PRM

Usual weights plus alterations at right

| | | |
|---|---|---|
| Average $P_{CC}$ = | +3 | Sect 1, CL3&4-1 |
| Average $P_{CC}$ = | -10 | Sect2, CL3&4-1 |
| Average $P_{CC}$ = | +11 | Sect 3, CL1-1, CL2-2 |
| Average $P_{CC}$ = | +12 | |
| Average $P_{CC}$ = | +10 | |
| Average $P_{CC}$ = | +3 | |
| Average $P_{CC}$ = | +11 | |
| Average $P_{CC}$ = | +1 | |
| AVG. = | +5 | |

36. [LPEELE.FLIGHT.FILES]LPTRAIN_ANGSECT2.PRM

Baseline classifier gains

| | | |
|---|---|---|
| Average $P_{CC}$ = | +5 | |
| Average $P_{CC}$ = | -7 | Sect1 IF O/E > 2. |
| Average $P_{CC}$ = | +13 | O/W Sect2 IF std < 2.95 |
| Average $P_{CC}$ = | +15 | O/W Sect3 IF std > 2.95 |
| Average $P_{CC}$ = | +11 | Sect3 CL1-1,CL2-2 |
| Average $P_{CC}$ = | +3 | Sect1&2 CL3-1 |
| Average $P_{CC}$ = | +10 | |
| Average $P_{CC}$ = | +0 | |
| AVG. = | +6 | |

37. [LPEELE.FLIGHT.FILES]LPTRAIN42_ANGSECT.PRM

| | | |
|---|---|---|
| Average $P_{cc}$ = | +1 | D2 Wavelet 42 |
| Average $P_{cc}$ = | -9 | Usual 3 std branches |
| Average $P_{cc}$ = | +13 | Usual biases in addition |
| Average $P_{cc}$ = | +14 | to original BL biases |
| Average $P_{cc}$ = | +12 | (see below for details) |
| Average $P_{cc}$ = | +2 | |
| Average $P_{cc}$ = | +8 | |
| Average $P_{cc}$ = | -1 | |
| AVG. = | +5 | |

38. [LPEELE.FLIGHT.FILES]LPTRAIN42_ANGSECT.PRM

| | | |
|---|---|---|
| Average $P_{cc}$ = | +3 | D2 Wavelet 42 & BL biases |
| Average $P_{cc}$ = | -6 | Sect1 IF O/E > 2.0 |
| Average $P_{cc}$ = | +14 | Sect2 IF NOT1 & std < 2.95 |
| Average $P_{cc}$ = | +17 | Sect3 IF NOT1 & std > 2.95 |
| Average $P_{cc}$ = | +14 | Sect1&2 CL3-1 |
| Average $P_{cc}$ = | +4 | Sect3 CL1-1,CL2-2 |
| Average $P_{cc}$ = | +7 | |
| Average $P_{cc}$ = | -1 | |
| AVG. = | +7 | |

**METHOD 2 SCORING RESULTS**

39. BASELINE CLASSIFIER GAINS

Average $P_{CC}$ = +6

Average $P_{CC}$ = -7

Average $P_{CC}$ = +3

Average $P_{CC}$ = +6

Average $P_{CC}$ = +10

Average $P_{CC}$ = +1

Average $P_{CC}$ = +5

Average $P_{CC}$ = -2

AVG. = +3 (+2.8)

Sample size weighted average of merged class 3 $P_{CC}$ values = - 0.2

40. [LPEELE.FLIGHT.FILES]TRAIN_BL_ANG_TT.PRM

Average $P_{CC}$ = +5

Average $P_{CC}$ = -5

Average $P_{CC}$ = +10

Average $P_{CC}$ = +6

Average $P_{CC}$ = +9

Average $P_{CC}$ = +3

Average $P_{CC}$ = +1

Average $P_{CC}$ = -5

AVG. = +3

Turntable data for training using only those aspects of flight training data

41. [LPEELE.FLIGHT.FILES]TRAIN_BL_ANG.PRM

Average $P_{CC}$ = +6

Average $P_{CC}$ = -8

Average $P_{CC}$ = +6

Average $P_{CC}$ = +3

Average $P_{CC}$ = +11

Average $P_{CC}$ = +2

Average $P_{CC}$ = +5

Average $P_{CC}$ = -4

AVG. = +3

Turntable training data at flight training aspects plus flight training data

42. BASELINE CLASSIFIER GAINS, THEN MERGED CLASS 3 FORCED INTO CLASS 1

| | | |
|---|---|---|
| Average $P_{CC}$ = | +11 | |
| Average $P_{CC}$ = | -4 | This illustrates why $P_{CC}$ values should |
| Average $P_{CC}$ = | +26 | not be averaged based on |
| Average $P_{CC}$ = | +17 | relative sample sizes. (That is, |
| Average $P_{CC}$ = | +15 | since there were relatively few |
| Average $P_{CC}$ = | +11 | class 3 test cases, this score |
| Average $P_{CC}$ = | +1 | looks good.) |
| Average $P_{CC}$ = | -3 | |
| AVG. = | +9 | |

43. CLASSIFIER GAINS: 0.00 0.00 0.00 0.00

| | |
|---|---|
| Average $P_{CC}$ = | -6 |
| Average $P_{CC}$ = | -15 |
| Average $P_{CC}$ = | -9 |
| Average $P_{CC}$ = | -1 |
| Average $P_{CC}$ = | +5 |
| Average $P_{CC}$ = | -4 |
| Average $P_{CC}$ = | +2 |
| Average $P_{CC}$ = | -6 |
| AVG. = | -4 |

44. [LPEELE.FLIGHT.FILES]TRAIN_W48.PRM NO WEIGHTS (ALL ZERO

| | |
|---|---|
| Average $P_{CC}$ = | -9 |
| Average $P_{CC}$ = | -15 |
| Average $P_{CC}$ = | 1 |
| Average $P_{CC}$ = | +1 |
| Average $P_{CC}$ = | +8 |
| Average $P_{CC}$ = | +1 |
| Average $P_{CC}$ = | +1 |
| Average $P_{CC}$ = | -1 |
| AVG. = | -2 |

45. [LPEELE.FLIGHT.FILES]TRAIN_W48.PRM  WEIGHTS = BL WEIGHTS

Average $P_{cc}$ = +3

Average $P_{cc}$ = -6

Average $P_{cc}$ = +8

Average $P_{cc}$ = +9

Average $P_{cc}$ = +11

Average $P_{cc}$ = +4

Average $P_{cc}$ = +5

Average $P_{cc}$ = -1

AVG. = +4

46. [LPEELE.FLIGHT.FILES]TRAIN_W26.PRM (**.25)

Weights = baseline weights

Average $P_{cc}$ = -4

Average $P_{cc}$ = -10

Average $P_{cc}$ = -1

Average $P_{cc}$ = +5

Average $P_{cc}$ = +8

Average $P_{cc}$ = -3

Average $P_{cc}$ = +0

Average $P_{cc}$ = -2

AVG. = -1

47. [LPEELE.FLIGHT.FILES]TRAIN_W42_FROOT.PRM (**.25)

Weights = baseline weights

Average $P_{cc}$ = +4

Average $P_{cc}$ = -6

Average $P_{cc}$ = +4

Average $P_{cc}$ = +8

Average $P_{cc}$ = +11

Average $P_{cc}$ = +2

Average $P_{cc}$ = +3

Average $P_{cc}$ = -1

AVG. = +3

48. [LPEELE.FLIGHT.FILES]TRAIN_W42.PRM

Weights = Baseline Average $P_{CC}$ = + 2

Average $P_{CC}$ = - 7

Average $P_{CC}$ = + 5

Average $P_{CC}$ = + 8

Average $P_{CC}$ = +12

Average $P_{CC}$ = + 3

Average $P_{CC}$ = + 6

Average $P_{CC}$ = + 1

AVG = + 4

49. [LPEELE.FLIGHT.FILES]TRAIN_W42_TT_ONLY.PRM

Train on TT only, weights = baseline

Average $P_{CC}$ = -14

Average $P_{CC}$ = -14

Average $P_{CC}$ = - 5

Average $P_{CC}$ = + 1

Average $P_{CC}$ = +13

Average $P_{CC}$ = + 0

Average $P_{CC}$ = + 2

Average $P_{CC}$ = - 5

AVG. = - 2

50. [LPEELE.FLIGHT.FILES]TRAIN_W42_F_ONLY.PRM

Train on flight only, weights = baseline

Average $P_{CC}$ = + 8

Average $P_{CC}$ = - 2

Average $P_{CC}$ = +16

Average $P_{CC}$ = + 7

Average $P_{CC}$ = +12

Average $P_{CC}$ = + 8

Average $P_{CC}$ = + 5

Average $P_{CC}$ = - 9

AVG. = + 6

This improvement is a fiction due to sample test weights - results are worse in equal $P_{CC}$ class weighting (see 9)

51. [LPEELE.FLIGHT.FILES]TRAIN_BL_SP_INDEP.PRM

| | | |
|---|---|---|
| Average $P_{CC}$ = | +5 | |
| Average $P_{CC}$ = | -7 | Independent clutter addition to |
| Average $P_{CC}$ = | +4 | turntable data for training |
| Average $P_{CC}$ = | +5 | |
| Average $P_{CC}$ = | +8 | |
| Average $P_{CC}$ = | +1 | |
| Average $P_{CC}$ = | +3 | |
| Average $P_{CC}$ = | -3 | |
| AVG. = | +2 | |

52. [LPEELE.FLIGHT.FILES]TRAIN_BL_SP.PRM

| | | |
|---|---|---|
| Average $P_{CC}$ = | +3 | |
| Average $P_{CC}$ = | -7 | |
| Average $P_{CC}$ = | +7 | Dependent clutter addition |
| Average $P_{CC}$ = | +9 | to turntable data for training |
| Average $P_{CC}$ = | +9 | |
| Average $P_{CC}$ = | +1 | |
| Average $P_{CC}$ = | +5 | |
| Average $P_{CC}$ = | -2 | |
| AVG. = | +3 | |

53. [LPEELE.FLIGHT.FILES]TRAIN_BL_SP_TT.PRM

| | | |
|---|---|---|
| Average $P_{CC}$ = | -3 | |
| Average $P_{CC}$ = | -12 | |
| Average $P_{CC}$ = | +1 | Same as case 52 except |
| Average $P_{CC}$ = | -1 | train only on turntable data |
| Average $P_{CC}$ = | +11 | |
| Average $P_{CC}$ = | +0 | |
| Average $P_{CC}$ = | +2 | |
| Average $P_{CC}$ = | -5 | |
| AVG. = | -1 | |

54. [LPEELE.FLIGHT.FILES]LPTRAIN_BL_ANG.PRM

Average Pcc = + 6

| | | |
|---|---|---|
| Average $P_{CC}$ = | -6 | This is trained on flight |
| Average $P_{CC}$ = | +14 | training files and turntable |
| Average $P_{CC}$ = | +10 | training data from similar |
| Average $P_{CC}$ = | +7 | aspects - uses only 1 sector |
| Average $P_{CC}$ = | -1 | |
| Average $P_{CC}$ = | +7 | |
| Average $P_{CC}$ = | +3 | |
| AVG. = | +5 | |

55. [LPEELE.FLIGHT.FILES]LPTRAIN_BL_ANG_TT.PRM

| | | |
|---|---|---|
| Average $P_{CC}$ = | -2 | |
| Average $P_{CC}$ = | -6 | Same as case 54 except |
| Average $P_{CC}$ = | +10 | trained only on |
| Average $P_{CC}$ = | +10 | turntable data at |
| Average $P_{CC}$ = | +5 | flight training angles |
| Average $P_{CC}$ = | -1 | |
| Average $P_{CC}$ = | +3 | |
| Average $P_{CC}$ = | -3 | |
| AVG. = | +2 | |

56. [LPEELE.FLIGHT.FILES]LPTRAIN_BL.PRM

| | | |
|---|---|---|
| Average $P_{CC}$ = | +2 | |
| Average $P_{CC}$ = | -5 | One sector only |
| Average $P_{CC}$ = | +13 | |
| Average $P_{CC}$ = | +14 | |
| Average $P_{CC}$ = | +6 | |
| Average $P_{CC}$ = | +0 | |
| Average $P_{CC}$ = | +4 | |
| Average $P_{CC}$ = | +2 | |
| AVG. = | +5 | |

57. [LPEELE.FLIGHT.FILES]LPTRAIN_BL_TT.PRM

| | | |
|---|---|---|
| Average $P_{CC}$ = | -4 | |
| Average $P_{CC}$ = | -7 | Train on turntable only |
| Average $P_{CC}$ = | +8 | Use only one sector |
| Average $P_{CC}$ = | +11 | |
| Average $P_{CC}$ = | +6 | |
| Average $P_{CC}$ = | -3 | |
| Average $P_{CC}$ = | +2 | |
| Average $P_{CC}$ = | -3 | |
| AVG. = | +1 | |

58. [LPEELE.FLIGHT.FILES]TRAIN_BL_TT.PRM

| | | |
|---|---|---|
| Average $P_{CC}$ = | -5 | |
| Average $P_{CC}$ = | -10 | Baseline |
| Average $P_{CC}$ = | +1 | Train on turntable only |
| Average $P_{CC}$ = | +3 | |
| Average $P_{CC}$ = | +9 | |
| Average $P_{CC}$ = | -1 | |
| Average $P_{CC}$ = | +4 | |
| Average $P_{CC}$ = | -2 | |
| AVG. = | +0 | |

59. [LPEELE.FLIGHT.FILES]LPTRAIN_W42.PRM

| | | |
|---|---|---|
| Average $P_{CC}$ = | -1 | |
| Average $P_{CC}$ = | -4 | One sector only |
| Average $P_{CC}$ = | +12 | |
| Average $P_{CC}$ = | +13 | |
| Average $P_{CC}$ = | +9 | |
| Average $P_{CC}$ = | -1 | |
| Average $P_{CC}$ = | +3 | |
| Average $P_{CC}$ = | +1 | |
| AVG. = | +4 | |

60. [LPEELE.FLIGHT.FILES]LPTRAIN_W48.PRM

| | | |
|---|---|---|
| Average $P_{CC}$ = | +3 | |
| Average $P_{CC}$ = | -6 | One sector only |
| Average $P_{CC}$ = | +14 | |
| Average $P_{CC}$ = | +14 | |
| Average $P_{CC}$ = | +7 | |
| Average $P_{CC}$ = | +0 | |
| Average $P_{CC}$ = | +5 | |
| Average $P_{CC}$ = | +3 | |
| AVG. = | +5 | |

61. [LPEELE.FLIGHT.FILES]LPTRAIN_W42_REG.PRM

| | | |
|---|---|---|
| Average $P_{CC}$ = | -1 | |
| Average $P_{CC}$ = | -4 | Second registration used, |
| Average $P_{CC}$ = | +11 | one sector only |
| Average $P_{CC}$ = | +10 | |
| Average $P_{CC}$ = | +10 | |
| Average $P_{CC}$ = | -1 | |
| Average $P_{CC}$ = | +3 | |
| Average $P_{CC}$ = | +1 | |
| AVG. = | +4 | |

62. [LPEELE.FLIGHT.FILES]PROFILE.PRM

| | | |
|---|---|---|
| Average $P_{CC}$ = | 6 | Profile-match |
| Average $P_{CC}$ = | -14 | Profile match baseline except used |
| Average $P_{CC}$ = | -7 | 4th root then normed by sqrt of |
| Average $P_{CC}$ = | +3 | sum of squares |
| Average $P_{CC}$ = | -4 | |
| Average $P_{CC}$ = | -13 | |
| Average $P_{CC}$ = | -2 | |
| Average $P_{CC}$ = | -8 | |
| AVG. = | -6 | |

63. [LPEELE.FLIGHT.FILES]PROFILE.PRM

Class 1 has a bias of +0.001

| | | |
|---|---|---|
| Average $P_{cc}$ = | +8 | |
| Average $P_{cc}$ = | -8 | |
| Average $P_{cc}$ = | +14 | Same as case 62 except |
| Average $P_{cc}$ = | +16 | for the +0.001 class 1 bias |
| Average $P_{cc}$ = | +8 | |
| Average $P_{cc}$ = | +0 | |
| Average $P_{cc}$ = | +7 | |
| Average $P_{cc}$ = | +2 | |
| AVG. = | +6 | |

64. [LPEELE.FLIGHT.FILES]PROFILE.PRM

Class 1 has +0.0007 bias

| | | |
|---|---|---|
| Average $P_{cc}$ = | +7 | |
| Average $P_{cc}$ = | -10 | |
| Average $P_{cc}$ = | +9 | Same as case 62 except |
| Average $P_{cc}$ = | +15 | class 1 has a +0.0007 bias |
| Average $P_{cc}$ = | +5 | |
| Average $P_{cc}$ = | -4 | |
| Average $P_{cc}$ = | +6 | |
| Average $P_{cc}$ = | +0 | |
| AVG. = | +4 | |

65. [LPEELE.FLIGHT.FILES]PROFILE_TT.PRM, CLASS 1 BIAS IS +.001, TRAIN ON TURNTABLE ONLY

| | | |
|---|---|---|
| Average $P_{cc}$ = | +5 | |
| Average $P_{cc}$ = | -11 | |
| Average $P_{cc}$ = | +10 | Same as case 63 except |
| Average $P_{cc}$ = | +8 | train on turntable only |
| Average $P_{cc}$ = | +8 | |
| Average $P_{cc}$ = | -1 | |
| Average $P_{cc}$ = | +5 | |
| Average $P_{cc}$ = | -2 | |
| AVG. = | +3 | |

66. [LPEELE.FLIGHT.FILES]LPTRAIN_W42.PRM - USUAL BIAS WEIGHTS, ALSO USES PROFILE.PRM, FUSE CLASSIFIER

PM class 1 has +0.001 bias

| | | |
|---|---|---|
| Average $P_{CC}$ = | +9 | |
| Average $P_{CC}$ = | -4 | Fusion classifier - fusion criterion is |
| Average $P_{CC}$ = | +16 | to use quadratic with usual weights |
| Average $P_{CC}$ = | +19 | unless (BDNEXT - BDMIN) < 2 ; then |
| Average $P_{CC}$ = | +10 | use profile matching. Currently |
| Average $P_{CC}$ = | +0 | there is no logic in the branching |
| Average $P_{CC}$ = | +6 | test for handling CL3 & CL4 merge |
| Average $P_{CC}$ = | +5 | |
| AVG. = | +8 | |

67. [LPEELE.FLIGHT.FILES]LPTRAIN_W42.PRM , ALSO USES PROFILE.PRM, FUSE CLASSIFIER

| | | |
|---|---|---|
| Average $P_{CC}$ = | +9 | |
| Average $P_{CC}$ = | -5 | Same as case 66 except |
| Average $P_{CC}$ = | +16 | < 2 is changed to < 2.8 |
| Average $P_{CC}$ = | +18 | |
| Average $P_{CC}$ = | +9 | This will use quadratic classifier |
| Average $P_{CC}$ = | +0 | approximately 1/2 of the time |
| Average $P_{CC}$ = | +8 | |
| Average $P_{CC}$ = | +5 | |
| AVG. = | +8 | |

68. [LPEELE.FLIGHT.FILES]LPTRAIN_W42.PRM

USUAL BIAS WEIGHTS ALSO USES PROFILE.PRM, FUSE CLASSIFIER,

Class 1 has +0.001 bias

| | | |
|---|---|---|
| Average $P_{CC}$ = | +8 | |
| Average $P_{CC}$ = | -3 | Uses PM (not QD) if |
| Average $P_{CC}$ = | +16 | 2500*PM_DELTA |
| Average $P_{CC}$ = | +18 | is > Q_DELTA; |
| Average $P_{CC}$ = | +10 | 2500 is approximately the |
| Average $P_{CC}$ = | +0 | ratio of median deltas |
| Average $P_{CC}$ = | +8 | PM_DELTA / Q_DELTA |
| Average $P_{CC}$ = | +5 | |
| AVG. = | +8 | |

69. [LPEELE.FLIGHT.FILES]LPTRAIN_W42.PRM -

USUAL BIAS WEIGHTS ALSO USES PROFILE.PRM, FUSE CLASSIFIER

Class 1 has +0.001 bias

Average $P_{CC}$ = +9

Average $P_{CC}$ = -3 Selects class based on

Average $P_{CC}$ = +18 minimum across classes of

Average $P_{CC}$ = +19 (QUAD BD + [(1-PM#)*2500])

Average $P_{CC}$ = +12 where the quad BD and the

Average $P_{CC}$ = +3 PM# are from the same class

Average $P_{CC}$ = +8

Average $P_{CC}$ = +5

AVG. = +9 (+ 8.9)

70. [LPEELE.FLIGHT.FILES]LPTRAIN42_ANGSECT.PRM FUSED WITH PROFILE MATCHING WITH T+0.001

Fusion is by minimum of (Q + 2500(1-PM))

Baseline classifier gains

Sectors are: Sect1 if O/E > 2.

Sect2 if not1 and std < 2.95

Sect3 if not1 and std > 2.95

Extra biases are Sect1&2 CL3-1, Sect3 CL1-1, CL2-2

This classifier has the best M1 and M2 results.

Average $P_{CC}$ = +8

Average $P_{CC}$ = -1

Average $P_{CC}$ = +17

Average $P_{CC}$ = +20

Average $P_{CC}$ = +12

Average $P_{CC}$ = +2

Average $P_{CC}$ = +9

Average $P_{CC}$ = +5

AVG. = +9 (+ 9.0)

Sample size weighted average of merged class 3 $P_{CC}$ values = - 12.8

71. [LPEELE.FLIGHT.FILES]LPTRAIN42_ANGSECT.PRM & PROFILE.PRM ( FUSION) SECTORS ARE: SECT1 IF O/E > 2.

[PM (not fusion) used in Sect3], Sect2 if not1 and std < 2.95, Sect3 if not1 and std > 2.95, baseline classifier gains, extra quadratic biases are Sect2 CL3&4-1, CL2+2; Sect3 CL1-1, CL2-2; profile matching biases are CL1+0.001, CL3+0.0005; BD(i) = QD(i) and BB(i) = (1 -PM(i))*2500 for i =1,...,4; then BD(3) = min(BD(3), BD(4)) & BB(3) = min(BB(3), BB(4)) [merges CL4 into CL3]; fuse by min of 3 classes BD(1)+BB(1)-0.5, BD(2)+BB(2), BD(3)+BB(3)-1.

This classifier has good class 3 $P_{CC}$ and good M1 & M2 results.

Average $P_{CC}$ = +4

Average $P_{CC}$ = -2

Average $P_{CC}$ = +10

Average $P_{CC}$ = +14

Average $P_{CC}$ = +10

Average $P_{CC}$ = -1

Average $P_{CC}$ = +8

Average $P_{CC}$ = +5

AVG. = +6

Sample size weighted average of merged class 3 $P_{CC}$ values = -0.2

72. DIAGONAL COVARIANCE Q - 90 SECTORS [POOR RESULTS]

73. DIAGONAL COVARIANCE Q - 90 SECTORS - **.25 NORMALIZATION [BETTER, NOT GOOD]

Below results have class 1 bias - 5

Average $P_{CC}$ = +3

Average $P_{CC}$ = -7

Average $P_{CC}$ = +2

Average $P_{CC}$ = +14

Average $P_{CC}$ = +7

Average $P_{CC}$ = -2

Average $P_{CC}$ = +1

Average $P_{CC}$ = -4

AVG. = +2

74. [LPEELE.FLIGHT.FILES]LPTRAIN_ANGSECT.PRM – 3 SECTORS BASED ON EVEN ST.DEV. STATISTIC (EVEN F(I)/|F|) CLASSIFIER GAINS ALTERED SLIGHTLY FOR 3 SECTOR ST.DEV. DIST.'S, BASELINE CLASSIFIER GAINS PLUS ALTERATIONS

| | | |
|---|---|---|
| Average $P_{CC}$ = | +2 | Three sectors A, B, C are |
| Average $P_{CC}$ = | -3 | A if std < 2.65 |
| Average $P_{CC}$ = | +12 | B if 2.65 < std < 2.95 |
| Average $P_{CC}$ = | +14 | C if 2.95 > std |
| Average $P_{CC}$ = | +8 | A bias is CL3-1 |
| Average $P_{CC}$ = | -1 | C biases are CL1-1, CL2-2 |
| Average $P_{CC}$ = | +9 | |
| Average $P_{CC}$ = | +3 | |
| AVG. = | +6 | |

75. [LPEELE.FLIGHT.FILES]LPTRAIN_ANGSECT.PRM

USUAL WEIGHTS PLUS ALTERATIONS AT RIGHT

| | | |
|---|---|---|
| Average $P_{CC}$ = | -1 | Sect1, CL3&4-1 |
| Average $P_{CC}$ = | -3 | Sect 2, CL3&4-1 |
| Average $P_{CC}$ = | +10 | Sect3, CL1-1 |
| Average $P_{CC}$ = | +12 | CL2-2 |
| Average $P_{CC}$ = | +8 | |
| Average $P_{CC}$ = | -1 | |
| Average $P_{CC}$ = | +8 | |
| Average $P_{CC}$ = | +1 | |
| AVG. = + 4 | | |

76. [LPEELE.FLIGHT.FILES]LPTRAIN_ANGSECT2.PRM

BASELINE CLASSIFIER GAINS

| | | |
|---|---|---|
| Average $P_{CC}$ = | -1 | |
| Average $P_{CC}$ = | -2 | Sect1 if O/E > 2. |
| Average $P_{CC}$ = | +11 | Otherwise Sect2 if std < 2.95 |
| Average $P_{CC}$ = | +15 | or Sect3 if std > 2.95 |
| Average $P_{CC}$ = | +8 | Sect3 biases CL1-1, CL2-2 |
| Average $P_{CC}$ = | -1 | Sect1&2 CL3-1 |
| Average $P_{CC}$ = | +7 | |
| Average $P_{CC}$ = | +0 | |
| AVG. = | +5 | |

77. [LPEELE.FLIGHT.FILES]LPTRAIN42_ANGSECT.PRM

| | | |
|---|---|---|
| Average $P_{cc}$ = | -3 | D2 Wavelet42 |
| Average $P_{cc}$ = | -5 | Usual 3 std branches |
| Average $P_{cc}$ = | +11 | Usual biases in addition to |
| Average $P_{cc}$ = | +14 | the original BL biases |
| Average $P_{cc}$ = | +10 | |
| Average $P_{cc}$ = | -2 | |
| Average $P_{cc}$ = | +7 | |
| Average $P_{cc}$ = | +0 | |
| AVG. = | +4.0 | |

78. [LPEELE.FLIGHT.FILES]LPTRAIN42_ANGSECT.PRM

| | | |
|---|---|---|
| Average $P_{cc}$ = | +0 | D2 Wavelet42 & BL biases |
| Average $P_{cc}$ = | -2 | Sect1 if O/L > 2.0 |
| Average $P_{cc}$ = | +12 | Sect2 if not1 & std < 2.95 |
| Average $P_{cc}$ = | +16 | Sect3 if not1 & std > 2.95 |
| Average $P_{cc}$ = | +10 | Sect1&2 CL3-1 |
| Average $P_{cc}$ = | +0 | Sect3 CL1-1, CL2-2 |
| Average $P_{cc}$ = | +7 | |
| Average $P_{cc}$ = | -1 | |
| AVG. = | +5 | |

## REFERENCES


[1] R. Coifman, Y. Meyer, and M.V. Wickerhauser, "Wavelet Analysis and Signal Processing, Wavelets and Their Applications," ed. Ruskai, et. al., ISBN 0-86720-225-4, Jones and Bartlett, Boston, 1992, pp. 153-178

[2] Ronald R. Coifman and M.V. Wickerhauser, "Entropy Based Methods for Best Basis Selection," IEEE Transactions on Information Theory, March 1992

[3] C. K. Chui, "An Introduction to Wavelets," Academic Press, New York

[4] I. Daubechies, "Orthonormal Bases of Compactly Supported Wavelets," Communications in Pure Applied Mathematics, Vol. 41, November 1988, pp. 909-996

[5] I. Daubechies, "Ten Lectures on Wavelets," CBMS-NSF Series in Applied Mathematics, SIAM Publications, Philadelphia, 1992

[6] T. H. Einstein, "Generation of High Resolution Range Profiles and Range Profile Auto-Correlation Functions Using Stepped-Frequency Pulse Trains," Project Report TT-54 prepared for DARPA under Contract F19628-85-C-002, 18 October 1984

[7] D. Gabor, "Theory of Communication," Journal of the IEE, Vol. 93, 1946, pp. 429-457

[8] S. Mallat, "Multiresolution Approximations and Wavelet Orthonormal Bases on L2 (R)," Trans. Amer. Soc., June 1989.

[9] S. Mallat, "A Theory for Multiresolution Signal Decomposition: the Wavelet Representation," IEEE Transactions on Pattern Analysis and Machine Intelligence, Vol. 11, No. 7, July 1989, pp. 674-693

[10] Rioul O., and Veteri, M., "Wavelets and Signal Processing," IEEE Signal Processing Magazine, Vol. 8, No. 4, October 1991, pp. 14-38

[11] Smith, M. J., and Barnwell, T. P., "Exact Reconstruction Techniques for Tree-Structured Subband Coders, IEEE Transactions on ASSP 34, 1986, pp. 434-441

[12] G. Strang, "Wavelets and Dilation Equations: A Brief Introduction," SIAM Review, Vol. 31-4, 1989, pp. 614-627

## REFERENCES


[1] R. Coifman, Y. Meyer, and M.V. Wickerhauser, "Wavelet Analysis and Signal Processing, Wavelets and Their Applications," ed. Ruskai, et. al., ISBN 0-86720-225-4, Jones and Bartlett, Boston, 1992, pp. 153-178

[2] Ronald R. Coifman and M.V. Wickerhauser, "Entropy Based Methods for Best Basis Selection," IEEE Transactions on Information Theory, March 1992

[3] C. K. Chui, "An Introduction to Wavelets," Academic Press, New York

[4] I. Daubechies, "Orthonormal Bases of Compactly Supported Wavelets," Communications in Pure Applied Mathematics, Vol. 41, November 1988, pp. 909-996

[5] I. Daubechies, "Ten Lectures on Wavelets," CBMS-NSF Series in Applied Mathematics, SIAM Publications, Philadelphia, 1992

[6] T. H. Einstein, "Generation of High Resolution Range Profiles and Range Profile Auto-Correlation Functions Using Stepped-Frequency Pulse Trains," Project Report TT-54 prepared for DARPA under Contract F19628-85-C-002, 18 October 1984

[7] D. Gabor, "Theory of Communication," Journal of the IEE, Vol. 93, 1946, pp. 429-457

[8] S. Mallat, "Multiresolution Approximations and Wavelet Orthonormal Bases on L2 (R)," Trans. Amer. Soc., June 1989.

[9] S. Mallat, "A Theory for Multiresolution Signal Decomposition: the Wavelet Representation," IEEE Transactions on Pattern Analysis and Machine Intelligence, Vol. 11, No. 7, July 1989, pp. 674-693

[10] Rioul O., and Veteri, M., "Wavelets and Signal Processing," IEEE Signal Processing Magazine, Vol. 8, No. 4, October 1991, pp. 14-38

[11] Smith, M. J., and Barnwell, T. P., "Exact Reconstruction Techniques for Tree-Structured Subband Coders, IEEE Transactions on ASSP 34, 1986, pp. 434-441

[12] G. Strang, "Wavelets and Dilation Equations: A Brief Introduction," SIAM Review, Vol. 31-4, 1989, pp. 614-627